SYNTHESIS OF MESOPOROUS SILICA PARTICLES USING SDS-PLURONIC COUPLES

A THESIS

SUBMITTED TO THE DEPARTMENT OF CHEMISTRY

AND THE INSTITUTE OF ENGINEERING AND SCIENCES

OF BILKENT UNIVERSITY

IN PARTIAL FULFILLMENT OF THE REQUIREMENTS

FOR THE DEGREE OF

MASTER OF SCIENCE

By

MUSTAFA SAYIN

July 2010

I certify that I have read this thesis and that in my opinion is it is fully adequate, in scope and quality, as a thesis of the degree of Master in Science

…….

Prof. Dr. Ömer Dağ (Supervisor)

I certify that I have read this thesis and that in my opinion is it is fully adequate, in scope and quality, as a thesis of the degree of Master in Science

…….

Assoc. Prof. Dr. Margarita Kantcheva

I certify that I have read this thesis and that in my opinion is it is fully adequate, in scope and quality, as a thesis of the degree of Master in Science

…….

Assist. Prof. Dr. Erman Bengü

I certify that I have read this thesis and that in my opinion is it is fully adequate, in scope and quality, as a thesis of the degree of Master in Science

…….

Assist. Prof. Dr. Emrah Özensoy

I certify that I have read this thesis and that in my opinion is it is fully adequate, in scope and quality, as a thesis of the degree of Master in Science

…….

Assist. Prof. Dr. Emren Nalbant Esentürk

I certify that I have read this thesis and that in my opinion is it is fully adequate, in scope and quality, as a thesis of the degree of Master in Science

…….

Prof. Dr. Levent Onural

Director of Institute of Engineering and Science

ABSTRACT

SYNTHESIS OF MESOPOROUS SILICA PARTICLES USING SDS-PLURONIC COUPLES

MUSTAFA SAYIN

M.S. in Chemistry

Supervisor: Prof. Dr. Ömer Dağ

July, 2010

Controlling the cooperative self assembly and micellization of pluronics and SDS (sodium dodecyl sulfate)are pivotal for the synthesis of mesoporous silica particles. The pH and temperature of the synthesis media, SDS/Pluronic mole ratio, TMOS (tetramethyl orthosilicate)amount, alkali salt amount of the synthesis solution are the parameters, which play significant roles on the micellization and self assembly of surfactants. The synthesis of mesoporous silica particles with distinct morphologies is possible with the precise optimizations of these parameters.

In this thesis we have investigated the synthesis of mesoporous silica particles with a well defined morphology and structure using SDS-Pluronic couple as the template. The pore size can be tuned by changing the aggregation number of the surfactant

molecules in the micelles, also by changing the pluronic type. The morphological control is achieved mainly by changing the pH and temperature of the synthesis media. At different temperatures and pHs, rods, spheres, muffin and 's' shaped particles have been obtained. The addition of inorganic salts, such as $NaNO_3$, NaCl, and KCl, has also effects on the morphology and meso-structure. Addition of a small amount of $NaNO_3$ changes spherical particles to amorphous silica however, addition of large amount of $NaNO_3$ gives well defined muffin shaped and worm-like particles. The concentration of nitrate ion also affects the pore size and wall thickness of the synthesized particles. The KCl or NaCl salts also have similar effects on the morphology of the silica particles, the morphological transitions have been observed but the role of Cl^- ion is minor on the control of pore size.

The SDS concentration has important effects on the micellization of pluronics, changing the SDS/Pluronic mole ratio (between 0.05 and 5.0) in the reaction media changes the structure of the mesoporous silica particles. Particularly the SDS concentration has important effects on the surface area of the synthesized particles. The surface area of the samples changes between 100 m^2/g and 700 m^2/g and the pore size of the particles changes between 3.0 and 6.0 nm by changing the SDS/Pluronic mole ratio. This ratio is also effective on the micropore amount of the samples together with mesopores. The tunable particle size (between 0.2μ to 1000μ) and morphology (spheres, rods, muffin and 's' shaped.) can be achieved by changing the SDS concentration.

Furthermore, the low reaction temperature (below RT) is essential for the synthesis of mesoporous silica particles in SDS-Pluronic system. However, the low

temperature is a problem for micellization. This problem was overcome by using P123, which has low critical micellization concentration (CMC) and critical micellization temperature (CMT) values or by using Hofmeister ions to decrease the pluronic surfactant solubility and the CMC and CMT of the pluronics used. Decreasing solubility of the pluronics causes effective micellization of the surfactants. The well defined micelles are the templates for the synthesis of mesoporous silica particles.

Overall , the effects of SDS/Pluronic mole ratio, pH and temperature of the synthesis solution, TMOS concentration, and the additives (alkali salts) have been investigated by synthesis of more than 300 samples that were analyzed using PXRD, SEM, TEM, POM, and N_2 sorption techniques.

Keywords: Mesoporous silica, SDS, Pluronics, Micellization, Morphology control, Silica rods, Salt effect.

ÖZET

MEZO YAPILI SİLİKA PARÇACIKLARININ SDS-PLURONIC İKİLİSİ İLE SENTEZİ

MUSTAFA SAYIN

Kimya Yüksek Lisans Tezi

Danışman: Prof. Dr. Ömer Dağ

Temmuz, 2010

Pluronik ve SDS yüzeyaktiflerinin kendiliğinden bir araya gelme ve misel oluşturma özelliklerinin kontrolü, mezo gözenekli silika parçacıklarının sentezinde en etkili ve önemli basamaktır. Yüzeyaktiflerin misel oluşturma özellikleri, ortamın pH'sına ve sıcaklığına, ortamdaki TMOS miktarına, bazı inorganik tuzların yoğunluğuna ve SDS/Pluronic mol oranına bağlı olarak kontrol edilebilinir. Farklı morfolojilerdeki silika parçacıklarının sentezi, yukarıda bahsi geçen parametrelerin hassas optimizasyonu ile mümkün olmuştur.

Bu tezde, SDS-Pluronik yüzeyaktif sistemini kullanarak, çok iyi tanımlanmış morfoloji ve yapılarda mezogözenekli parçacıkların sentezini detaylı olarak çalışıldı. Yüzeyaktiflerin türünün ve misele katılım sayılarının değiştirilmesiyle, silika parçacıklarının gözenek yarıçapları; sıcaklık ve pH'nin değiştirilmesiyle de morfolojileri kontrol edildi. Farklı sıcaklık ve pH değerlerinde; çubuk, küre, topaç ve

"s" şeklinde parçacıkların sentezi kaydedilmiştir. Ortama ayrı ayrı eklenen, $NaNO_3$, KCl ve NaCl anorganik tuzlarının morfolojiye ve mezoyapıya etkileri saptanmıştır. $NaNO_3$ ün reaksiyon ortamına eklenmesi radikal morfolojik değişimlere sebep olmuş, artan $NaNO_3$ konsantrasyonu küre şeklindeki parçacıkların önce amorf silikaya dönüşmesine ancak konsantrasyonun daha da artmasıyla parçacıkların topaç şekline ve "s" şekline benzer morfolojiler kazanmasına neden olmuştur. $NaNO_3$ ün oratamdaki konsatrasyonu, parçacıkların gözenek yarıçapı ve duvar kalınlıklarını da etkiler. KCl veya NaCl tuzlarının varlığı da $NaNO_3$ e çok benzer etkiler göstermiş ancak bu tuzların varlığı genelde morfolojik geçişlerde etkili olmuş, mezoyapıda ve gözenek yapısında belirgin etkileri gözlenmemiştir.

SDS konsantrasyonun, pluronik yüzeyaktiflerinin misel oluşturmasında ve oluşan miselin farklı özellikler taşımasında önemli etkileri vardır. SDS/Pluronic mol oranını değiştirerek (0,05 ve 5,0 arasında) parçacıkların yapıları değiştirilebilinir. Özellikle SDS yoğunluğu sentezlenen parçacıkların yüzey alanlarında önemli etkendir. Parçacıkların yüzey alanı SDS/Pluronik mol oranıyla bağlantılı olarak 100 m^2/g ve 700 m^2/g arasında değerler almıştır. Sentezlenen parçacıkların boyutu, yüzey alanı, gözenek hacmi ve morfolojisi SDS miktarı değiştirilerek sağlanabilir. Parçacıkların gözenek büyüklüğü de SDS yoğunluğunu değiştirerek kontrol edilmiştir (3,0 ve 6,0 nm arasında). Düşük sıcaklık, SDS-Pluronic sisteminde mezoyapılı silika parçacığı sentezlemede gereklidir. Fakat düşük sıcaklık miselleşmede problem oluşturur. Bu problem kritik misel sıcaklığı (KMS) ve kritik misel konsantrasyonu (KMK) düşük olan nötr yüzeyaktif, P123 kullanılarak veya yüzeyaktiflerin sudaki çözünürlüklerini; KMK ve KMS değerlerini düşüren Hoffmeister iyonları kullanılarak aşılmıştır.

Pluroniklerin çözünürlüğünü düşürmek, yüzeyaktiflerin etkili miselleşmesini sağlar. İyi tanımlanmış miseller, mezogözenekli silika parçacıkların sentezinde yönlendiricidirler.

Sonuç olarak, SDS/Pluronik mol oranı, sentez çözeltilerin pH ve sıcaklığı, TMOS yoğunluğu ve katkı maddelerinin (alkali tuzlar) etkileri; sentezlenen üçyüzden fazla numunenin PXRD, SEM, POM, TEM ve N_2 sorpsiyon teknikleri kullanılarak analizi sonucu gösterilmiştir

Anahtar kelimeler: Mezo yapılı silika, SDS, Pluronikler, Miselleşme, Morfolojik Kontrol, Silika Çubuklar, Tuz Etkileri

ACKNOWLEDGEMENT

It is a mere misunderstanding that the most easy-to-write section of a book is the acknowledgement. For my own part, I have never had feelings which I could not set down into words in such a difficult manner. It is hard to express my cordial appreciation for these who encouraged me in this work, because I always feel the emptiness in these sentences just says “Thank You”. I wish, at lest lyrically, I had the talent to express my great respect and love for the following people:

My supervisor Prof. Ömer Dağ who have always showed maximum support that a supervisor can. In my life I have met few people who had such a great patience and understanding.

My dearest friend Altuğ Poyraz, whose works in our lab enlightened our understanding in synthesis. In addition to his solid support in some of the experiments, he has always been one of the most prewment source of the positive atmosphere in my life for the last 11 years.

Cemal Albayrak is one of those guys that can rarely had chance to meet in their lifes. I have always appreciated our long talks in which we were able to discuss almost about anything as if both of us were the only polymaths of the 21st century. He also had great solid help in this work.

All the remaining members of our chemistry department who had created a nice atmosphere for me to be here for the last 7 years.

I cannot find the words to express my love for Kübra Demirel and my family. I feel as if I am dissolved in their love completely and I can’t think about myself without them.

Table of Contents

LIST OF TABLES

LIST OF FIGURES

INTRODUCTION

Developments in the fields of separation, drug delivery, catalysis, and nanodevices, have impact on the ordered porous materials, which have tunable pore structures with a unique particle morphology [1-4]. The pore size of a few nanometers has a chance to meet the requirements for the applications that involve large molecules, for instance, biological and petroleum products [3, 4]. The ability to control the pore and morphology motivate to scientist to discover new classes of porous materials.

The porous solids can be classified in three groups, mainly, according to their pore size: microporous (pore diameter less than 2 nm), mesoporous (pore diameter between 2 to 50 nm) and macroporous (pore diameter larger than 50nm). The most important family of the microporous materials are the zeolites, which have crystalline structure. The zeolites that have perfect pore structures are used in various industries [4, 5]. The structural properties of zeolites enable these materials to have ion exchange capabilities and catalytic properties [4-6]. Additionally the hydrophilic and hydrophobic character of the inorganic zeolitic structures give to these materials the property of being specific adsorbents for the organic molecules. The major applications of the microporous zeolitic materials vary from adsorption to drying, catalysis to detergency [4-6]. Microporous materials have channels and cavities that are less than 2 nm open through to external medium [1, 4, 6]. The pore size of less than 2 nm is suitable for small molecular assemblies, but not suitable for the macro molecular assemblies. The dimensions and accessibility of pores are limited to sub-nanometers and this situation restricts the applications of these pore structures to small molecules [4, 6-9]. The morphology of the mesostructured silicates can be controlled as spheres, fibers, thin films and monoliths [6, 10-13].

The synthesis of first mesoporous particles was proposed by Pillard and coworkers in 1980s. However, their rectangular pore structure was not suitable for applications. Because the pores were not totally open, such that the reagents and products could not penetrate through the pores [4, 14-16]. The first mesoporous materials have a very wide pore size distribution and disordered pore arrangements. Early 1990s, Mobil company scientists reported the first ordered and open mesoporous silica [4, 14-16]. The first synthesis has been carried out by using cationic surfactant, cethyltrimethyl ammonium bromide (CTAB), as a template to obtain highly ordered mesoporous silica molecular sieves under hydrothermal basic conditions [12, 17].

The new materials were promising and attractive for applications, due to their 2-50 nm uniform pore size. These new materials also initiated the concepts of templating and open and tunable pore systems that provide convenience for modification[6, 18] . Additionally, the mesoporous materials have large surface area ($1500 m^2/g$), and highly ordered nanochannels [4, 6, 10-12, 19]. The first classes of mesoporous materials (M41S) are two dimensional (2D). hexagonal (MCM-41), a cubic (MCM-48) and lamellar structures such as MCM-50 [2, 4, 6, 7, 16]. Short after the first synthesis, the mesoporous materials with many different mesostructures have been synthesized, such as 3D-hexagonal (*P*63/*mmc)*, 3D cubic (*Pm*3h*m*, *Pm*3h*n*, *Fd*3h*m*, *Fm*3h*m*, *Im*3h*m)*, bicontinuous cubic (*Ia*3h*d)* and 2D-hexagonal (*p*6*mm)*, etc [4, 12, 18, 19].

The designing complex inorganic and hybrid materials are possible by controlling morphology, and construction hierarchy. Towards these goals, the silica based materials were investigated the most. Because the accurate control of condensation and hydrolysis reactions and a great thermal stability make silica

materials convenient for modifications that enhance their applications in the fields of catalysis, drug delivery, optics, electronics and adsorption, etc [1-3, 6].

After the invention of ordered mesoporous materials with silica precursors, many studies have been devoted to extend mesoporous materials to non-silicate materials. Many mesostructured phosphates and oxides of transition metals have been demonstrated [6]. These materials are motivating because of their structural properties that are important in many applications especially in catalysis, sensors, separation technologies, photocatalysis, etc [1-3, 6, 16]. Nevertheless, the reported studies and achievements in the transition metal materials are not yet as stimulating as in silicates.

The assembly of organic and inorganic species is determined by weak forces such as hydrogen bonding, van der Waals forces, and ionic interactions between the surfactant molecules and inorganic silica species [4, 6, 12, 20]. The cooperative self assembly of the surfactants and silica species result in forming mesostructured composites. The removal of the surfactants by calcination gives mesoporous molecular sieves [6, 21]. The control of surfactant self assembly is essential to obtain highly ordered mesostructures with various morphologies.

1.1 Synthesis Mechanism and Routes

Two main synthetic strategies has been established, which are effective in the synthesis of mesoporous structures, these are liquid-crystal templating process and cooperative self assembly processes, see Figure 1.1 [4, 7, 9, 15, 22]. The cooperative self assembly is based on the interactions between the surfactant micelles and silica species that form organic-inorganic mesostructured materials. The cooperative self assembly can be categorized into four stages, the adsorption of silicates on globular

micelles, the association of globular micelles into floes, the precipitation of floes, and the micelle-micelle coalescence [4, 6, 7, 18]. Khodakov suggested that hydrophobic PPO (polypropylene oxide) core of pluronic and hydrophilic PEO (poly ethylene oxide)-water slicate corona forms first, then the cylindrical micelles come together to form large domains [23]. Synchronously, the solvent molecules (water) are replaced with silicate species.

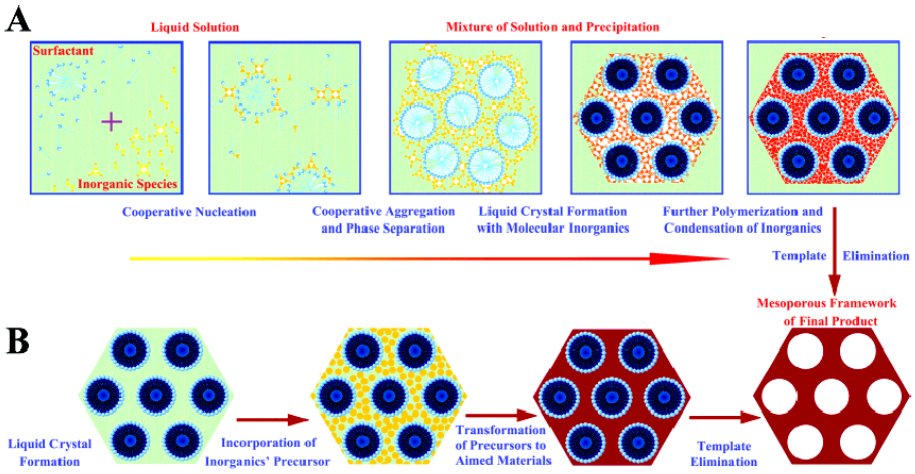

Figure 1.1: The two main pathways for synthesis of mesoporous materials: A) cooperative self assembly and B) liquid-crystal templating process, [4] (Reprinted with the permission of ACS.)

The formula of the free energy of this whole process has given by Monnier and Huo[4, 24]:

$$\Delta G = \Delta G_{inter} + \Delta G_{wall} + \Delta G_{intra} + \Delta G_{sol}$$

Where ΔG_{inter} is the energy related with the interaction between surfactant micelles and inorganic walls, ΔG_{wall} is the structural free energy change for the inorganic structures, ΔG_{intra} is the van der Waals force and conformational energy of the surfactant and ΔG_{sol} is the free energy related with the species in solution phase [4, 24].

For the cooperative self assembly of mesostructured silica particles ΔG_{sol} can be thought as constant on a given solution system. Therefore the important factor is the interactions of surfactants and silica species, for instance, matching of charge density. The assembly process can be carried easily if ΔG_{inter} is more negative [24]. Many studies have been carried to demonstrate the essentials of inorganic-organic interactions [4, 15, 18].

In the liquid crystalline templating pathway, the liquid crystalline phase is directly used to synthesize ordered mesoporous silica solids. The order and the mesostructure of the liquid crystal is mimicked by the inorganic precursors to obtain mesostructured films and monoliths [4, 15, 18, 22, 25]. Attard and co-workers have used high concentrations of nonionic surfactants as templates to synthesize ordered mesoporous silica. The condensation reactions of silica precursors around the surfactants, which were in the liquid crystal phase cause the formation of the mesostructured silica [25]. The confined growth of silica species around the surfactants formed the ceramic-like frameworks. The inorganic silica species get their pore structures, pore sizes, and symmetries from the LC scaffolds [25].

In the cooperative self assembly pathway generally hydrothermal method has been employed for the synthesis of mesoporous silica materials. In general, the procedure of the first step of this method is, preparing a homogenous solution by dissolving the surfactants in a solvent [4, 26, 27]. Water is mostly used as solvent in the synthesis. Then, the silica precursor is added to the reaction media, where the silica precursor undergoes hydrolysis and sol formation with the help of acid or base catalyst occurs[4, 26, 27]. The interactions between the surfactant micelles and silica oligomers, cooperative self assembly and the aggregation result in precipitation of mesostructured silica particles. To complete the condensation of silica and to enhance the meso-order, the hydrothermal treatment is usually employed [4, 26, 27]. At the end, the product is cooled down to room temperature (RT), washed and dried. Via calcination, the organic surfactants are removed to obtain mesoporous material [4, 6, 18, 21].

The pH of the solution is also very important because of its catalytic effect on the silica condensation. The extremely slow polymerization of silica precursors at neutral solutions makes difficult to synthesize mesoporous silica under neutral conditions, therefore the synthesis takes place usually under basic or acidic conditions [4, 6, 22, 28]. Fluoride ion can also be used as a catalyst in the synthesis of mesoporous materials [29-31].

The synthesis of mesoporous silica materials can be faciliated by decreasing pH of the solution [4, 6, 27, 28]. It has been investigated that the synthesis of mesoporous silica under acidic conditions enables diverse morphologies, for instance spheres, thin films, fibers, and single crystals, etc [10-13]. On the other hand, the morphology control for base catalyzed synthesis of mesoporous materials are quite difficult, because, there is no pH dependence of silica condensation under basic

conditions. Also the polymerization reaction of silicates is very fast, which results in 3D silicate networks[14, 32] . Moreover under the basic conditions, the spherical morphology is the common morphology.

In the presence of inorganic salts, such as $NaNO_3$, KCl, NaCl and Na_2SO_4 the synthesis of mesoporous materials can also be speeded up and improved, unlike organic solvents, which reduce the rate of hydrolysis and condensation of silica precursors [33-36]. The presence of inorganic salts also enables the synthesis at lower temperatures and lowers surfactant concentrations. It is also known that the presence of these salts improves the meso-order of the synthesized particles under some conditions [33-36].

The synthesis of mesoporous silica materials in aqueous solution can be carried out in a broad range temperatures, from -10 to 130^0C. The critical micellization temperature (CMT) and cloud-point (CP) determine the synthesis temperature range [4, 37-39]. To enhance the micellization, the temperature should be higher than the CMT and lower than the CP, because the surfactants form micelles above a certain surfactant concentration, below these point surfactant molecules are dissolved in the water and they are free molecules in the solution [37-39]. When the concentration of the surfactants are above the cloud point, at elevated temperatures, the surfactants molecules become insoluble in water, solution turns cloudy and they start to precipitate. The CMT values of the anionic and cationic surfactants are relatively low compared to the nonionic surfactants [20, 28, 37]. The assembly of the surfactants molecules into micelles can be controlled by controlling the temperature of the media. A high quality mesoporous silicate can be obtained at relatively low temperatures; under many conditions room temperature is convenient for the synthesis, and heating is not necessary. Because of the higher CMTs of the nonionic

surfactants (especially pluronics), the reaction temperature must be higher than RT therefore, heating may be needed for the pluronics [4, 6, 17, 36, 38, 39].

To enhance meso-order of the materials, the hydrothermal treatment step may be essential. The temperature, used in the hydrothermal treatment, is in the range of 80 to 150^0C. A temperature range of 95 to 100^0C is commonly used. This step that is employed after the formation of mesostructures to enhance the order in the materials may take place several days. [8, 28, 40].

The last step of mesoporous silica material synthesis is the removal of the surfactant templates. Many different removal techniques have been developed depending on the characteristics of the synthesized mesoporous materials. The most common method is calcination method. Extraction, high energy ultraviolet irradiation and utilized microwave irradiation are the other methods for the removal of the surfactant molecules from the mesoporous materials [4, 6].

In the calcination method, the temperature increment and the operation temperature is very important. Mobil company scientist proposed a two step calcination method to effectively remove the surfactants. They proposed 1 h heating under nitrogen atmosphere continuing 5 h under oxygen atmosphere, but this method is improved later and the nitrogen atmosphere step has been eliminated. The calcination, in an air atmosphere with a rate of 1^0C/min to 550^0C and keeping the samples at this temperature for about 4-6 hrs, totally removes the surfactant molecules [4, 6, 21, 40]. To determine the calcination temperature of the synthesized mesoporous materials and to ensure complete removal of surfactants , two major points should be considered, the temperature should be high enough for the decomposition of the surfactant template and low enough to prevent collapses of the

mesostructures. Also the calcination time and temperature should be set to an optimal value, because longer calcination time and temperatures result in lower surface area and lower pore volume [4, 41-43]. Another removal method for the surfactants is an extraction method, which is powerful when the mesostructures is sensitive, to heat treatment. Usually THF or ethanol are used as extracting agents. By this method, it has been reported that up to 95% of triblock copolymer can be removed [4, 6].

1.2 Surfactants and Micellization

The term surfactant was first used by Antara in 1950. Surfactants are usually organic molecules and have amphiphilic property. It means that they have both hydrophilic and hydrophobic parts in their structure. Because of this, the surfactant molecules is soluble in organic solvents and water [38, 44-46].

The amphiphilic properties of surfactant molecules enforce micellization in aqueous media above a critical concentration, known as critical micelle concentration (CMC). The micelles form, in water, by hiding the hydrophobic tails as a core and the hydrophilic head group forming a shell and contacting with aquous media [47-49]. In reverse micelles, which form in organic solvents, the hydrophilic head groups are in the core and the tail groups are in the outer shell of the micelles [42, 48, 49].

The surfactant molecules are classified mainly in three classes, which are non-ionic, anionic and cationic. The molecular structures of several types of surfactants are shown in Table 1.1 [4]. The surfactant systems are thermodynamically interesting and have special importance. Because the surfactant systems are stated as intermediate phases between an ordered and disordered state of matter [4, 6, 18]. For instance, free surfactant molecules form disordered phases, in contrast to micelles, which forms ordered structures.

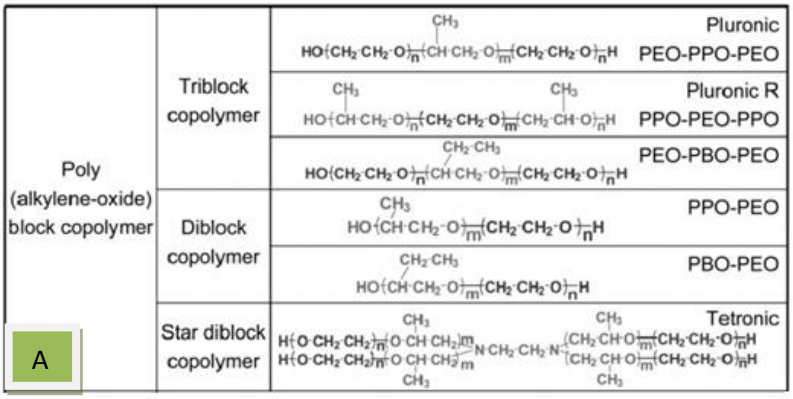

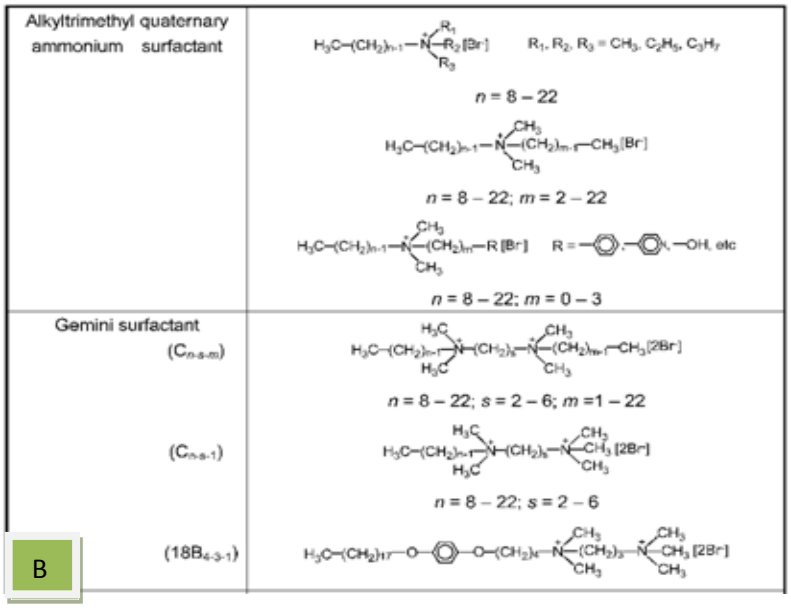

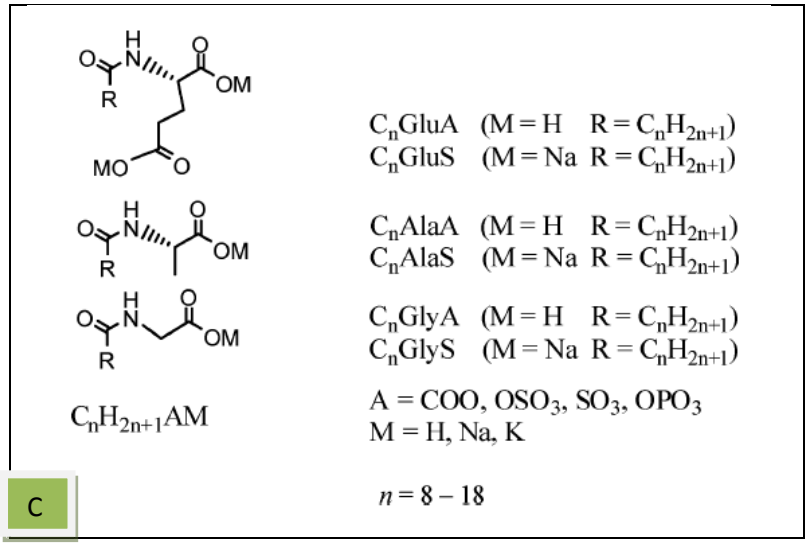

Table 1.1: The molecular structures of some of the known surfactants A) non-ionic B) cationic C) anionic [4].

The amphiphilic property of the surfactant molecules gives them a distinct solubility as compared to non-amphiphilic molecules. The surfactant molecules decrease the surface tension of water almost linearly with increasing surfactant concentration. At some point, the surface tension does not change much upon increasing surfactant concentration [18, 20, 44, 48]. Together with the surface tension, several other physical properties also show drastic changes such as, conductivity, turbidity, osmotic pressure and etc. All of these changes are related to the aggregation of surfactant molecules to form stable colloidal particles (aggregates), called micelles. While the hydrophilic part of the surfactant molecule is solvated by water molecules, the hydrophobic part disrupts the hydrogen-bonding network of water, therefore solubilization of the hydrophobic part is energetically unfavourable [50, 51]. At the same time, the aggregation of surfactant molecules is entropically unfavorable. At a certain concentration, called CMC (Critical Micellization Concentration), energetic contribution overcomes the entropy and surfactants start to form aggregates [50-52].

In this thesis, sodium dodecyl sulfate (SDS) has been used as anionic surfactant, which is also named as sodium lauryl sulfate or sodium laurilsulfate, see Figure 1.2. The main application of SDS is in the fields of cleaning and hygiene [53]. The molecular structure of SDS gives it a amphiphilic property because the molecule has a tail which consists of 12 carbon atoms attached to a sulfate head group. The hydrophilic and hydrophobic parts of SDS molecule make it a surfactant molecule and forms micelles in aqueous solution [54].

The non-ionic surfactants, used in this thesis are called poloxamers or pluronics, which are water soluble, ployethyleneoxide-ploypropyleneoxide-ployethyleneoxide (PEO-PPO-PEO), tri-block copolymers. The nonionic macromolecular surface-active

agents can be synthesized with different molecular weights and PPO/PEO composition ratios. The pluronics are used in industry in the fields of detergency, foaming, lubrication, emulsification, etc [39, 48, 50, 55]. The PPO blocks are in the core region and the PEO blocks are in the corana region of the micelle in aqueous media [39].

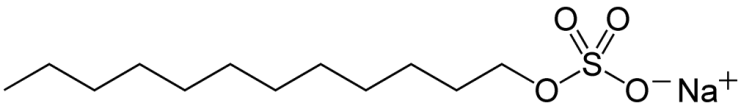

Figure 1.2: Sturucture of sodium dodecyl sulfate, ($NaC_{12}H_{25}SO_4$).

Types of surfactant molecule and its concentration, temperature, pH play significant roles on the shape and size of the micelles. By controlling these parameters the properties of the micelle can be controlled and modified [45, 48, 56-58]. In the literature, mixed surfactants have also been used to obtain micelles. For instance, SDS and several pluronics have been used together to obtain new properties. The long polymeric chains of the pluronics have been generally used to tune the micelle size and the anionic surfactant gives micelle a charged character [28, 44, 53].

1.3 Cooperative Assembly of SDS and Pluronics and Silica Particle Formation

The negatively charged SDS increases the solubility as a result the CMC of the pluronic surfactants. It is well known that the participation of SDS molecules with the pluronic micelles decreases the aggregation number of the micelles [44, 53, 59]. When SDS is at a certain concentration, SDS and pluronic surfactant molecules form mixed micelles. The critical concentration, where SDS aggregates together with pluronics to form micelles is relatively high, in contrast to cationic surfactants [4, 53]. Penetration of SDS molecules into the pluronic micelles is an exothermic process. Upon formation of SDS-pluronic micelles, the size and the aggregation number of the micelles decrease. The SDS-pluronic micelles have considerable charge, that cause repulsion among the micelles and affecting micelle concentration and aggregation number [53]. The addition of SDS molecules to the micellar solutions of pluronics has drastic changes on pluronic micelles. The core radius (R_c) and the hard-sphere radius (*R*hs) decrease gradually with increasing SDS concentrations, up to 1.0 SDS/Pluronic mole ratio, the amount of decrease in *R*c is considerably more than that in *R*hs [59]. The difference between the values of *R*c and *R*hs, which represents the shell thickness, increases upon addition of one SDS for each pluronic. This suggests that the PEO chains are extended in the corona region of the micelles in presence of SDS molecules. The raise in the shell thickness increases the volume fraction of the micelles which explains the observed increase in the micellar volume fraction is much higher. Because hydration of the micelles increases quite extensively in the existence of 1.0 SDS for each pluronic[59].

It is also evident that, although the micellar volume fraction first increases upon addition of SDS, it decreases with the following increase in the SDS concentration because of the reduction in the shell thickness [59, 60]. A higher rate of decrease of *R*hs as compared to that of *R*c leads to the observed decrease in the shell thickness. The triblock copolymer forms mixed micelles with SDS, and its aggregation number in the mixed micelles decreases with increasing SDS concentration [59-61]. The volume fraction of the micelles, however, increases significantly in the presence of SDS because of an increase in the degree of hydration of the micelles in the corona region. It has been suggested that the increased hydration of the micelles is achieved by stretching of the EO blocks in the corona region in the presence of SDS molecules [59-61]. Quite interestingly, the enhancement in micellar volume fraction upon addition of SDS leads to a marked increase in the stability of the micellar gel phase. It was found that the effect of SDS on the micellar structure and on the formation characteristics of the micellar gel phase depends strongly on the composition of the copolymer.

The schematic representation of cooperative self assembly of SDS and pluronic surfactants is shown in Figure 1.3.

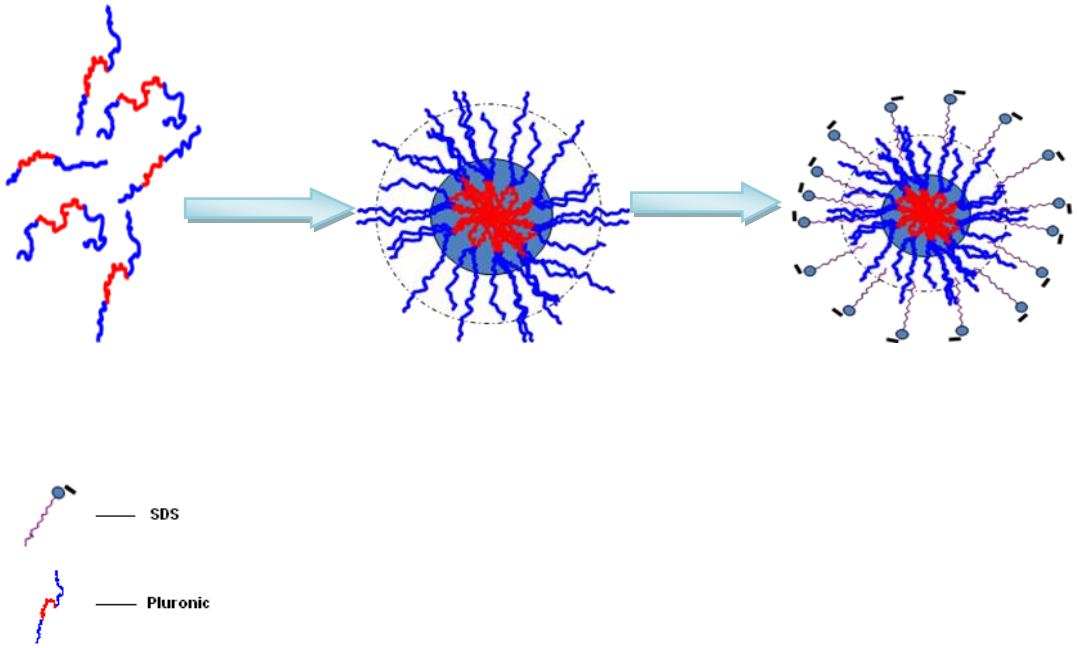

Figure 1.3: A schematic representation of the cooperative self-assembly of SDS and pluronic surfactant in the aqueous solution. The PEO groups of the copolymer is colored with blue and the PPO blocks colored with red.

The free pluronic molecules are shown on the left hand side of Figure 1.2. Above CMC, they start to form micelles. When there is enough SDS in the media, the SDS molecules locate themselves between the PEO blocks of the pluronics, at the corona region of the micelle. The presence of SDS enhances the hydration of the PEO-SDS and increase the volume in the corona region [59-61].

The effect of SDS on the micelle size, shape and charge density can be used as parameters in the synthesis of mesoporous silica particles. The tunable size and shape of the micelle by adding SDS is beneficial to obtain mesoporous silica with an adjustable pore size and pore structures. Also changing the charge density of the micelle changes the self assembly of the micelles and silica species, which lead to

synthesized silica particles with different morphologies and mesostructures. The rod shaped and spherical silica particles can be synthesized by manipulating the micelles. The manipulation and the modification of micelles can be done by several ways such as adjusting temperature and pH of the synthesis media, using co-surfactants and adjusting the surfactant concentration. By decreasing or increasing solubulities of the surfactants with these parameters, just mentioned before, the hydration of core and corona region can be controlled. Therefore, by controlling the amount of co-surfactant SDS, different micelle shapes can be obtained with various aggregation numbers and shapes, see Figure 1.3.[4, 6, 59]

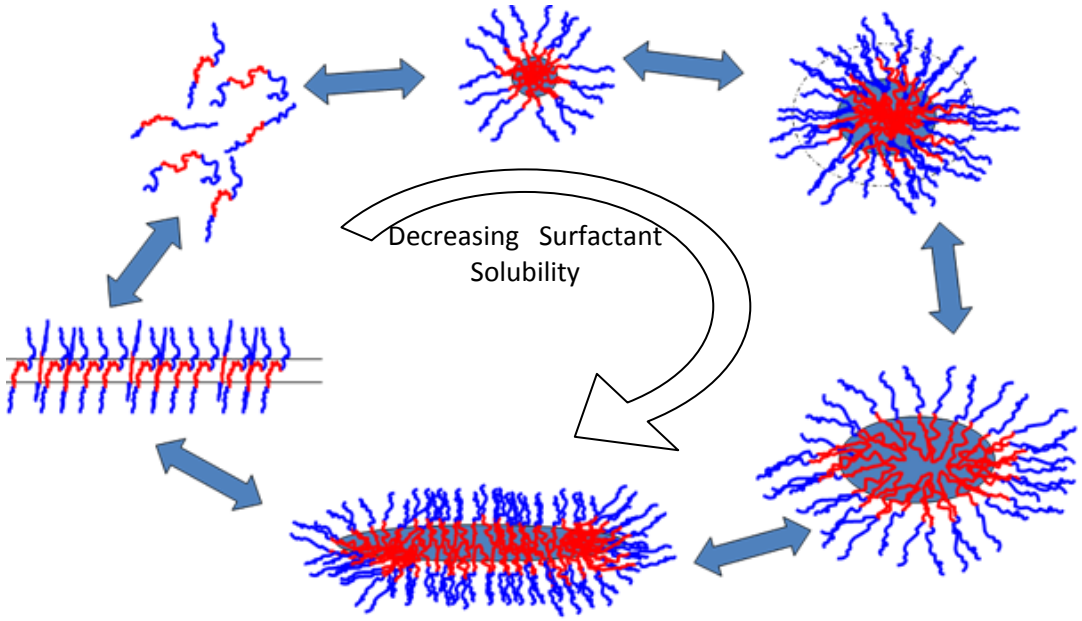

Figure 1.3: The scheme of micellar shape change related to decreasing solubility of surfactants.

Decreasing solubility of surfactants leads the formation of spherical micelles and further decrease of the surfactant solubility results in an increase of the aggregation number in the micelles. After this point, the micelles become egg shaped and the hydration of the core decreases. Decreasing the solubility of surfactant molecules

increases the aggregation number. Further decreasing the solubility causes the formation of elongated and bilayered micelles, which supplies efficient packing of high concentration of surfactant.

2. EXPERIMENTAL

2.1 Materials

All chemicals and solvents were reagent grade and used without any further purification.

Surfactants:	Company	M.W. (g/mol)	Molecular Formula
SDS	**Aldrich**	**288.38**	**$NaC_{12}H_{25}SO_4$**
P65	**BASF**	**3400**	**$EO_{20}PO_{30}EO_{20}$**
P103	**BASF**	**4950**	**$EO_{17}PO_{55}EO_{17}$**
P123	**Aldrich**	**5750**	**$EO_{20}PO_{70}EO_{20}$**

(EO= $-CH_2CH_2O-$; PO= $-CH_2(CH_3)CH_2O-$)

Salts:	Company	M.W. (g/mol)	Molecular Formula
Sodium Nitrate	**Panreac**	**84.99**	**$NaNO_3$**
Sodium Sulphate	**Carlo Erba**	**142.84**	**Na_2SO_4**
Sodium Fluoride	**Merck**	**41.99**	**NaF**
Potassium Chloride	**Merck**	**74.55**	**KCl**
Potassium Bromide	**Merck**	**119.01**	**KBr**
Potassium Iodide	**Merck**	**166.00**	**KI**

Other Chemicals:	Company	M.W. (g/mol)	Molecular Formula
TMOS (Tetramethyl Orthosilicate)	**Aldrich**	**152.22**	**$Si(OCH_3)_4$**
Sodium Hydroxide	**Riedel-de Haen**	**39.997**	NaOH
Hydrochloric Acid	**Riedel-de Haen**	**36.46**	HCl
Nitric Acid	**Riedel-de Haen**	**63.01**	HNO_3

2.2 Synthesis

2.2.1 Synthesis of Mesoporous Silica Particles using SDS and P123 at RT

Anionic surfactant, SDS and nonionic surfactant, P123 were mixed in an acidic media at different mole ratios. A stock solution was prepared by dissolving 15.6 g of P123 in 1 lt of deionized water (DI) and then stirring about 24 hours at room temperature (RT) to obtain a homogeneous solution. A 50 ml of the stock solution was diluted to 100 ml using DI. Then the anionic surfactant was added to the prepared solution at different SDS/P123 mole ratios (between 0 and 3.0). The mixture was stirred about 10 minutes with a magnetic stirrer. After the homogeneous solution was obtained, 1.0 ml TMOS (tetramethylorthosilicate) was slowly added to the solution and then vigorously stirred about 10 minutes at RT. The mixture was set for precipitation for 5 days in closed vessels at RT. The precipitates were filtered and washed using three portions of 50 ml DI. The powder samples were dried about 24 hours in a 50^0C oven. The dried samples were calcined by directly putting the

samples to 550^0C and kept for 5 hours, known as rapid calcination method (ref). In a typical synthesis, mole ratios of the chemicals are 1:2:48:74:41044 for P123:SDS:TMOS:HNO_3:H_2O, respectively[21].

2.2.2 Temperature Dependent Mesoporous Silica Particle Synthesis

The temperature dependent experiments were performed at temperatures 15^0C, 17^0C, 19^0C, 21^0C, 23^0C, 25^0C, 30^0C, 40^0C, 50^0C and 60^0C in temperature controlled oven at SDS/P123 mole ratios of 2.0, 1.8, 1.6, 1.4, 1.2, 1.0, 0.8, 0.6, 0.4, 0.2, 0.1, 0.05 and 0. A typical sample was prepared as following: A 50 ml stock solution of P123 was first diluted to 100 ml using DI at RT. To obtain pH 1.0, nitric acid was added drop by drop to the 100 ml pluronic solution by using a pH meter. Then 0.076 g of anionic surfactant was added to the solution and stirred about 10 minutes. Then the sample was aged at 23^0C for 3.0 hours to ensure thermal equilibrium. After thermal equilibrium was reached, 1.0 ml TMOS was added to the solution and the samples were set for precipitation for 5 days at 23^0C. The samples were filtered and washed with 3 portions of 50 ml DI. Then the powder samples were dried in a 50^0C oven for 24 hours. The dried samples were calcined using the rapid calcination method in air at 550 ^{0}C for 5.0 hours.

2.2.3 pH Dependent Mesoporous Silica Particle Synthesis

The pH dependent experiments were performed at pHs of 0.6, 0.8, 0.9, 1.0, 1.1, 1.5, 2.0, 3.0, 4.0, 4.5, 5.0, 5.5, 6.0, 7.0, 8.0, 9.0, 10.0 and 11.0 and SDS/P123 mole ratios of 2.0, 1.8, 1.6, 1.4, 1.2, 1.0, 0.8, 0.6, 0.4, 0.2, 0.1, 0.05 and 0. A typical sample was

prepared as follows: A 50 ml portions of the stock solution of the P123 was diluted to 100 ml by using DI. To obtain a desired pH, nitric acid was added drop by drop to the solution. The pH was controlled using a pH meter. Then 0.076g of SDS was added to the solution and stirred about 10 minutes at RT. 1.0 ml TMOS was added to the solution and the samples were set for precipitation for 5 days at RT. The samples were filtered and washed with 3 portions of 50 ml DI. Then they were dried in the 50^0C oven for 24 hours. The dried samples were calcined using the rapid calcination method in air at 550 ^{0}C for 5 hours.

2.2.4 Synthesis of Mesoporous Silica Particles in the Presence of Several Alkali Salts

The sample were prepared in the presence of some alkali salts such as $NaNO_3$, KI, NaF, KCl, KBr, Na_2SO_4 and SDS/P65 mole ratios of 2.0, 1.8, 1.6, 1.4, 1.2, 1.0, 0.8, 0.6, 0.4, 0.2, 0.1, 0.05 and 0 at RT. The alkali salts were added in the concentration range between 0.05M and 1.0 M. A typical sample was prepared as follows: 0.56 g of P65 was dissolved in the 50 ml DI and stirred about 10 minutes at RT. Then 0.038 g of anionic surfactant SDS was added to the above solution and stirred for another 10 minutes. Then 1.0 g of NaCl was added to the solution and stirred another 30 minutes. After getting a clear solution, pH was set by adding drop by drop concentrated HCl using a pH meter. 1.0 ml TMOS was added to the solution and the samples were set for precipitation for 2 days at RT. Then the samples were filtered, washed with 3 portions of 50 ml DI, and then dried in a 50^0C oven for 24 hours. The dried samples were calcined using the rapid calcination method in air at 550 ^{0}C for 5 hours.

2.3 Instrumentation

2.3.1 Powder X-Ray Diffraction

Powder X-Ray Diffraction (PXRD) Patterns were recorded on a Rigaku Miniflex diffractometer using Cu-Kα (λ=1.5405 Å) source operating at 30kV/15mA. The samples were packed in an aluminum sample holder and the PXRD patterns were collected in the 0.95-7 (2θ) range with 0.5^{o}/minute scan rate.

2.3.2 The Scanning Electron Microscopy

The SEM images were obtained by using ZEISS EVO-40. The SEM images were collected at 15 kV (EHT) operating voltage and 1.930 Å filament current. The powder samples were prepared on aluminum sample holders by dispersing small amount of powder samples using ethanol or acetone .

2.3.3 The N_2 Adsorption

TriStar 3000 automated gas adsorption analyzer (Micrometrics) was used to obtain the N_2 adsorption/desorption isotherms. Data were collected at a relative pressure range (P/P_0) from 0.01 to 0.99. Before measurements, the samples were dehydrated under vacuum (10^{-2} torr) for 3 hours at 350^{0}C in order to remove water and other volatile species adsorbed on the samples.

2.3.4 Polarized Optical Microscopy (POM)

The polarized optical microscopy (POM) images were recorded in transmittance mode on a ZEISS AXIO Scope A1 with reflected and transmitted light illumination, using white light between parallel and cross polarizers.

3. RESULTS AND DISCUSSION

Mesoporous silica can be obtained by using several methods. An important step in the formation of mesoporous particles is the aggregation of surfactant molecules into micelles before or during the assembly process of the micelles and silica species [22, 62-66]. Because of this, the method could also be named as micelle templated structure formation [46, 67, 68].

Surfactants, which are also named as structure directing agents could be mainly categorized into two different classes. The first class is neutral surfactants and the second one is charged surfactants. The crystal structure of the mesostructured silica depends on the surfactant type, organic and inorganic additives, and usage of co-solvent, temperature, pH and concentration of the ingredients. The slight changes in the conditions, mentioned above, play significant roles on the micellization and assembly properties of the surfactants, mesostructure and morphology of the silica particles.

In the literature, many surfactants have been used to improve the micellar phase and to obtain mesoporous silica materials. Assembly of mixed surfactants has been preferred in many studies, because the hybrid features of the surfactants make the modifications easier [69, 70]. The mixed surfactant systems could be obtained by using different types of surfactants such as neutral-cationic, neutral-cationic-anionic and neutral-anionic couples. There are many successful studies[1-4]using these surfactant systems to obtain mesoporous materials with different morphologies, modified surfaces and high surface areas. However, in the anionic-neutral surfactant

systems there are only a few studies that produce mesoporous silica with no well defined morphology. Although the anionic surfactants promise different morphologies, the anionic-neutral micellar system is quite difficult to study because of the high sensitivity to reaction conditions (temperature, pH, surfactant concentration, etc.).

In this study, the anionic-neutral mixed micellar system has been investigated by using sodium dodecylsulphate (SDS) as anionic surfactant and several types of pluronics (P123 and P65) as neutral triblock copolymer surfactants. The cooperative micellization properties of the pluronic surfactants with SDS are the key to synthesize mesostructured silica in this thesis. To overcome the difficulties of anionic-neutral system, which has been mentioned above and to achieve synthesis of mesoporous silica structures, appreciable amount of time has been devoted to systematically optimize reaction conditions. The parameters that are effective on the system are: SDS/Pluronic mole ratio, TMOS (silica source) amount, concentration of the surfactants, temperature, pH, inorganic additives, and pluronic surfactant type.

3.1 The Synthesis of Mesoporous Silica with SDS/P65 Surfactant System

In the light of already known procedures [65, 71-74] for the synthesis of mesoporous silica particles using cationic-neutral mixed surfactant systems and also making some modifications on these procedures, at first silica particles had been obtained by using SDS and P65. The following parameters; temperature, pH, and surfactant concentration need to be investigated. The initial temperature and pH were set to 90^0C and 0.9, respectively. However, these initial values of the temperature

and pH result in a complex and disordered morphology (Figure 3.1.1). Figure 3.1.3 shows two SEM images, recorded from those samples. Notice that the images do not display well defined shape. To understand and to obtain well defined particles, we have investigated the effect of temperature and pH on the synthesis of silica particles.

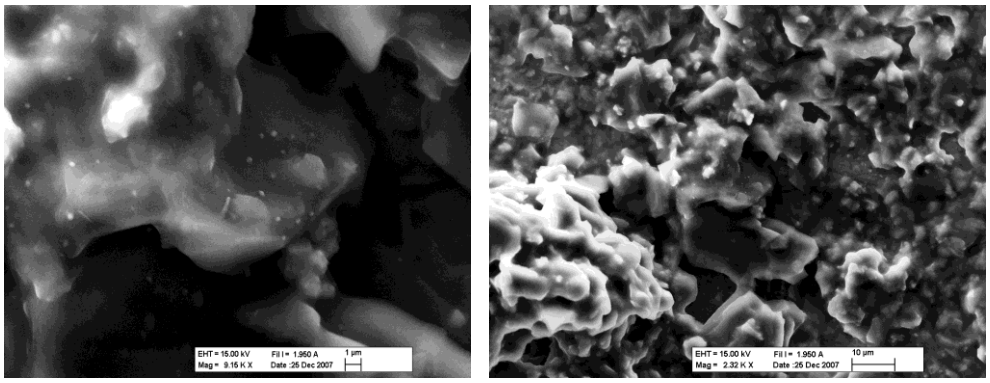

Figure 3.1.1: The SEM images of the silica particles obtained from the SDS-P65 system using SDS/P65 mole ratio of 3.0 at 90^0C and pH of 0.9.

3.1.1 The Effect of Temperature and pH on the Synthesis Silica Particles using SDS and P65

The temperature and pH have been optimized to obtain a mesoporous silica with a well defined shape from the SDS/P65 system. The pH values of 0.9, 1.0, 2.0, 3.0, 4.0, 5.0, 5.5, 6.0, 6.5, 7.0, 7.2, 7.5, 8.0, 8.5, 9.0, 9.5 and 10.0; and the temperatures values of 90^0C, 60^0C, 40^0C, 35^0C, 30^0C and 25^0C have used to synthesize silica particles. We found out that the synthesis of a desired morphology and ordered mesoporous silica particles are sensitive to temperature and pH of the synthesis media. Because the temperature and pH are both effective on the micellization of the surfactants and polymerization of the silica species.

Decreasing the reaction temperature to 60^0C and increasing pH to 2.0 resulted individual silica particles (see Figure 3.1.2) rather than amorphous undefined particles.

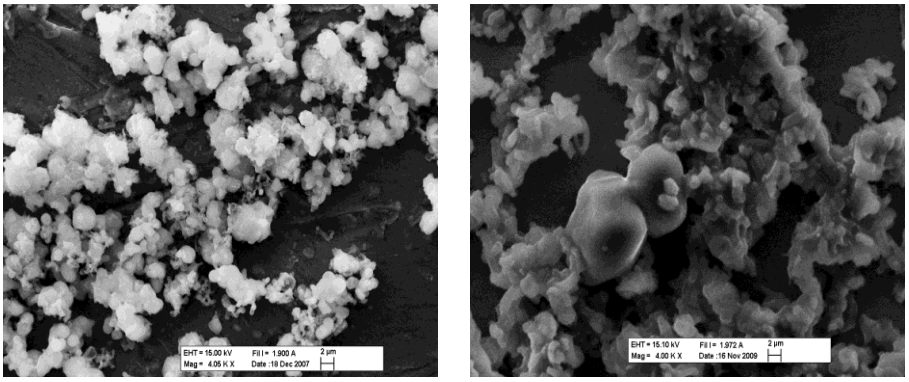

Figure 3.1.2: The SEM images of silica particles obtained from SDS-P65 system with SDS/P65 mole ratio of 3.0 at 60^0C and pH 2.0.

Many synthesis [1-4] have been carried out in a wide range of pH and temperature. These studies showed that, the pH interval of 4.0 to 8.5 was optimum with a temperature interval of 25^0C to 35^0C as well to obtain individual spherical silica particles. These studies also showed that the size distribution and the average size of the silica particles synthesized using SDS-P65 couples are pH sensitive at a constant temperature. Figure 3.1.3 shows the SEM images of the silica particles that the diameter of the silica spheres are under 1.0 μm and the shape of the particles is dominantly spherical. The SEM images of the particles, synthesized at pHs 4.5, 5.0 and 6.0 also show that the size distribution of the particles are very narrow, see Figure 3.1.3.

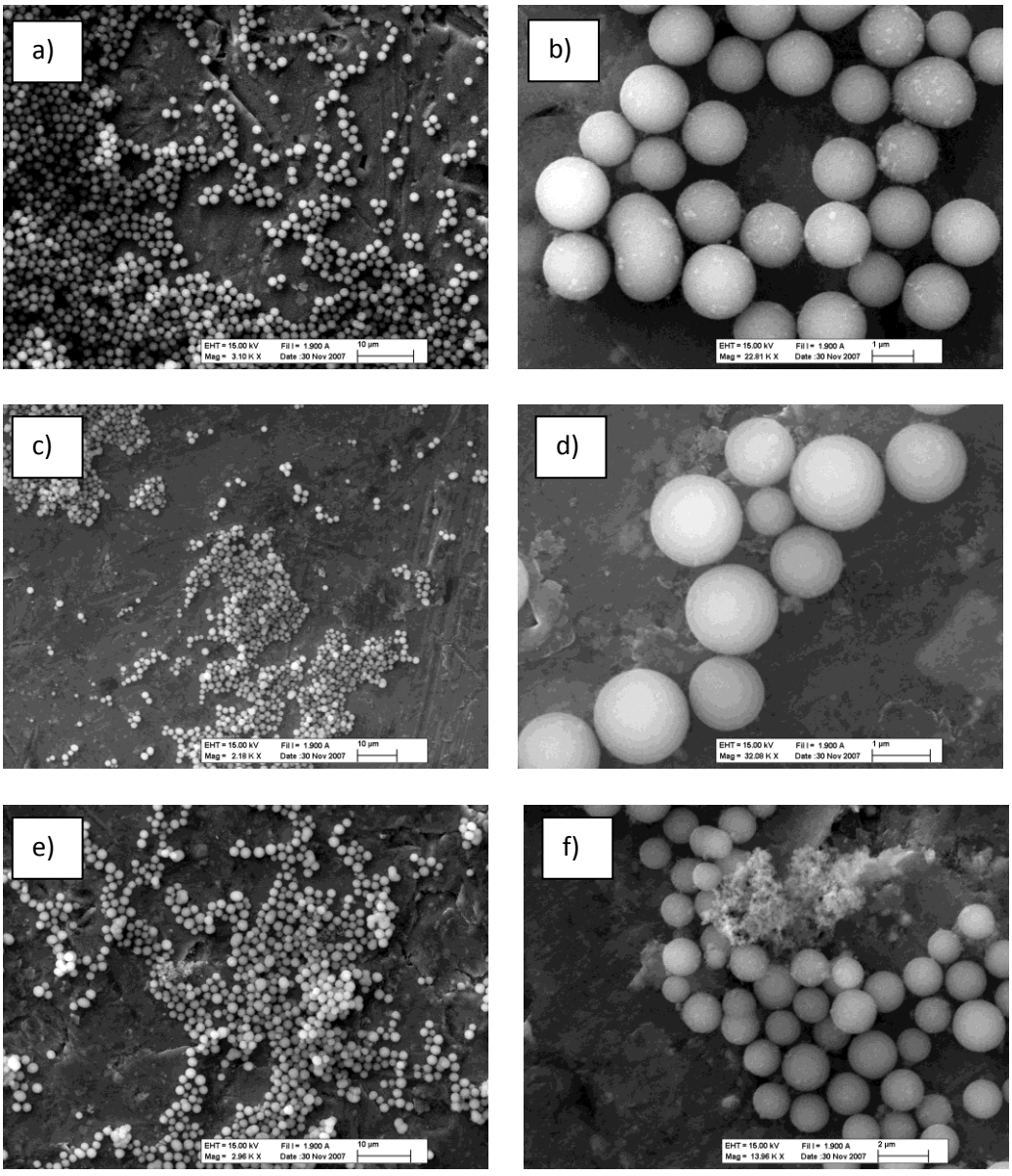

Figure 3.1.3: The SEM images of silica particles obtained from the SDS-P65 system using SDS/P65 mole ratio of 3.0 at 25^0C and pHs of a) 4.5, b) 4.5, c) 5.0, d) 5.0, e) 6.0 and f) 6.0.

The relationship between the particle size and the pH has been investigated and found out that the particle size could be tuned from 200 nm to 1000 nm by changing pH under our reaction conditions. Figure 3.1.4 shows the size distribution and changes of the silica particles with respect to pH. The average size of the spheres increases linearly from 200 nm to 1000 nm, when the pH is increased from 4.0 to 6.0

and then the average size starts to decrease from1000 nm to 300 nm, when the pH is increased from 6.0 to 7.2. In the basic media the average size is about 500 nm at a pH 9.5, see Figure 3.1.4.

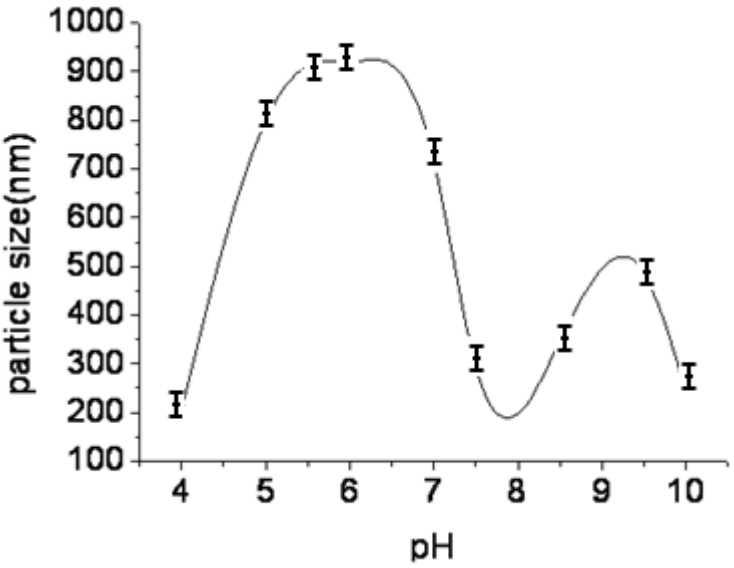

Figure 3.1.4: The average particle size versus pH plot of silica particles synthesized using SDS and P65 couple as a template.

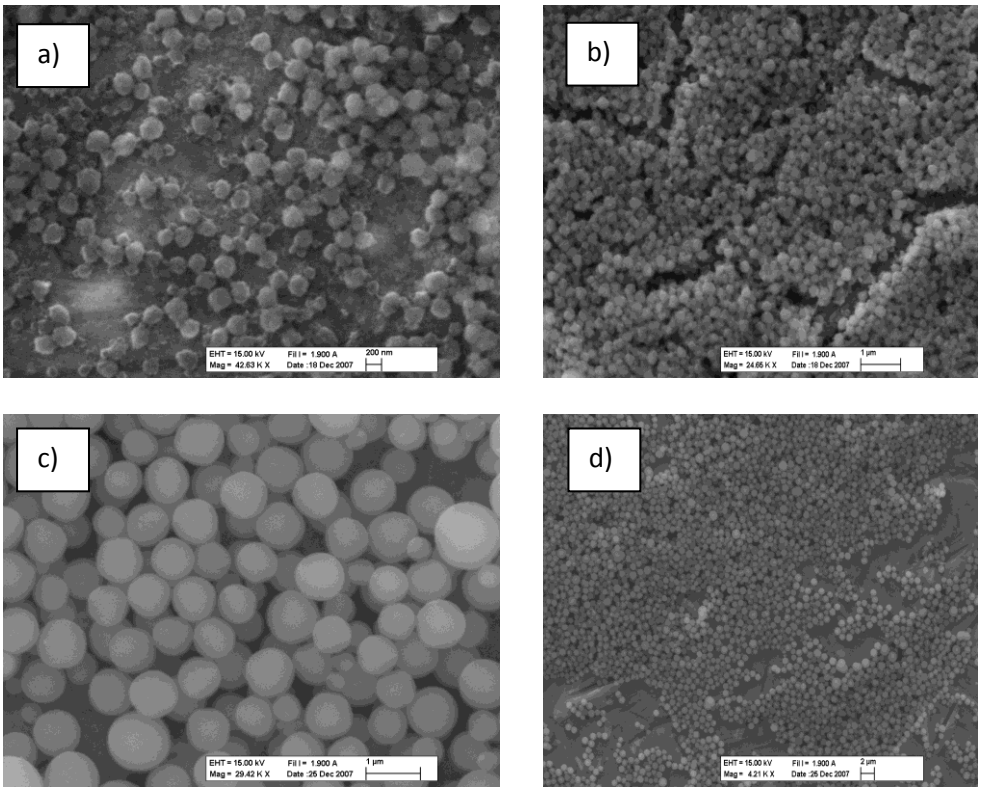

Figure 3.1.5: The SEM images of silica particles obtained from the SDS-P65 system with a SDS/P65 mole ratio of 3.0 at 25^0C and pHs of a)7.2, b)7.2, c)9.5, d)9.5

Although, the individual particles with a single morphology and uniform size were obtained, the PXRD data of the samples indicated that there is no meso-order in the samples. Also the N_2 sorption measurements showed that the synthesized particles have no mesoporocity. The N_2 adsorption-desorption isotherms, in Figure 3.1.6, show that the synthesized particles are microporous, with a typical type-I isotherm indicating microporous structure[78].

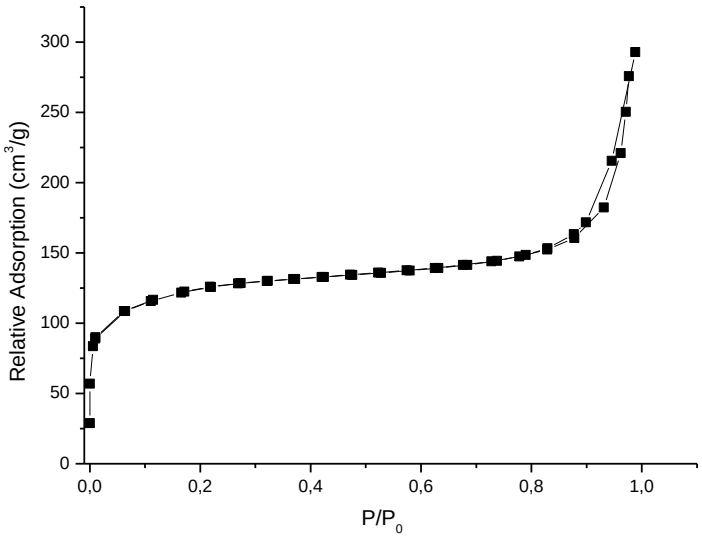

Figure 3.1.6: The N_2 adsorption-desorption isotherms at 77K of the silica particles, obtained using the SDS-P65 system with a SDS/P65 mole ratio of 3.0 at 25^0C.

Figure 3.1.7 shows the t-plot of the isotherm in Figure 3.1.6. Note that the downward deviation from the linearity of the t-plot is indicative of microporosity, (see Figure 3.1.7), rather than mesoporosity [78].

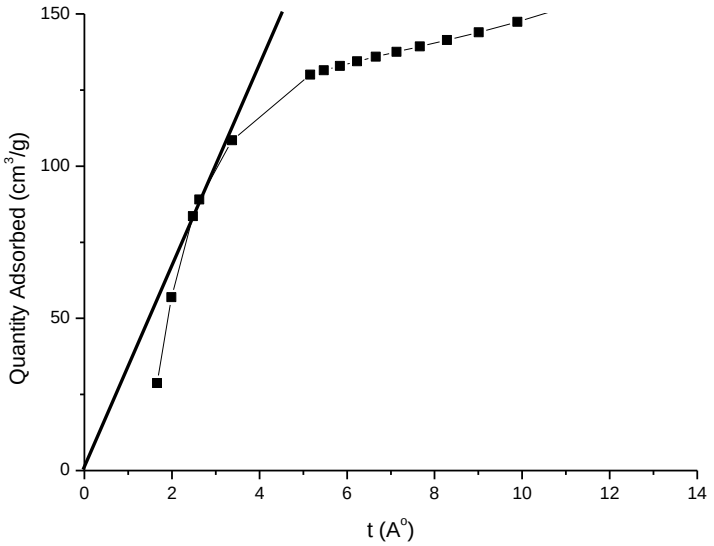

Figure 3.1.7: The t-plots obtain from the N_2 adsorption isotherms at 77 K of the silica particles, synthesized using SDS-P65 system with a SDS/P65 mole ratio of 3.0 at 25^0C.

Under our reaction conditions, discussed above, we have obtained uniform, well defined particles that did not have any mesoporosity. The likely reason for the lack of mesoporosity is the lack of formation of micelles under the reaction conditions. It is likely that the microporous silica forms by coating the EO blocks of the random P65 molecules. The microporous structure also indicates non-existence of the mixed micelles in the reaction media.

The pluronic surfactants form micelles above CMC and CMT. The micellization concentration of the surfactants decreases with increasing temperature. It means that increasing temperature increases the aggregation number of the surfactants and the number of micelles in the media. Therefore increasing temperature can be a solution for the micellization problem in the SDS-P65 system. However, temperature does not only play a role on the micellization, it has also an important effect on the

polymerization of silica. If the temperature is too high, the silica polymerizes too fast and cause gelation, which is the reason for formation of amorphous silica with an undefined morphology. Therefore, the key aspect for the synthesis of mesoporous silica particles with a well defined morphology, using anionic-neutral mixed surfactant system, is to find optimum conditions, which will enable an ideal micellization and silica polymerization. The (CMC) and (CMT) of the pluronic surfactants depend on the number of EO units and the molecular mass of the surfactants. In the SDS-P65 system, increasing temperature to enhance the micellization may not be a good solution, because fast polymerization of silica species above 40^0C, at pH ranges of 4.0 to 8.5, causes gel formation. Therefore, alternative approaches need to be developed.

3.1.2 The Effect of Chloride Ion in the Synthesis of Mesoporous Silica in SDS -P65 Surfactant System

The CMC of the pluronic surfactants could also be decreased by using alkali metal salts. The gelation problem of silica species may be overcome using alkali metal salts. It is known that these salts also have effects on the silica polymerization, however, the effect is much larger to micellization if it is used in ideal amounts. For instance NaCl can be used in SDS-P65 system to improve the micellization properties of these two surfactant couple for the synthesis of mesoporous silica particles. Therefore, NaCl salt is added to the reaction media with different mole ratios. The synthesis takes place about 24 hours without NaCl addition, however, when there is NaCl in the media the reaction time shortens to 40-80 minutes. This indicates that the Cl^- ion enhances the micellization, as a result, it leads to the

assembly and formation of mesostructured particles. Figure 3.1.8 shows the PXRD patterns of the samples, prepared using various amount of NaCl.

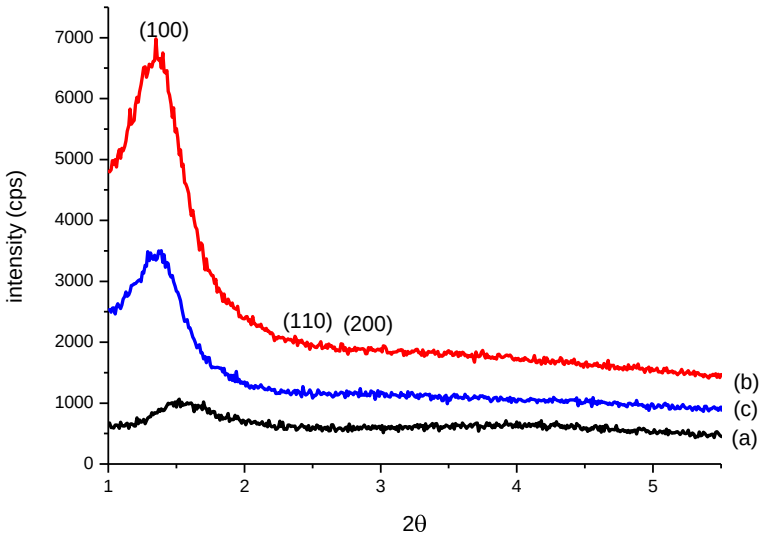

Figure 3.1.8: The PXRD patterns of the mesoporous silica particles obtained from the SDS-P65 system with a SDS/P65 mole ratio of 3.0, at pH 1.0 and NaCl concentration of (a) 0.25M, (b) 0.50M, and (c) 1.0M

The PXRD patterns, in Figure 3.1.8, clearly show that the meso-order increases with increasing NaCl concentration. The Peak at 1.37, 2θ is due to (100) planes of the 2D hexagonal structure. The broad feature between 2.0 and 4.0, 2 θ is due to (110) and (200) planes of the 2D hexagonal structure. It means that a regular cylindrical pore is forming under our reaction conditions. The unit cell dimension "a" ($a=d\sqrt{3}/2$) is equal to 65 Å.

The samples were further investigated using SEM technique. The SEM images show that the enhanced micellization leads to non-uniform spherical mesoporous silica particles. Figure 3.1.8 shows the SEM images of the silica particles,

synthesized at different NaCl concentrations. Remember that with no micelle formation, the silica particles precipitate with molecular surfactant species as microporous uniform silica spheres. However the micellization leads to non-uniform mesoporous silica spheres.

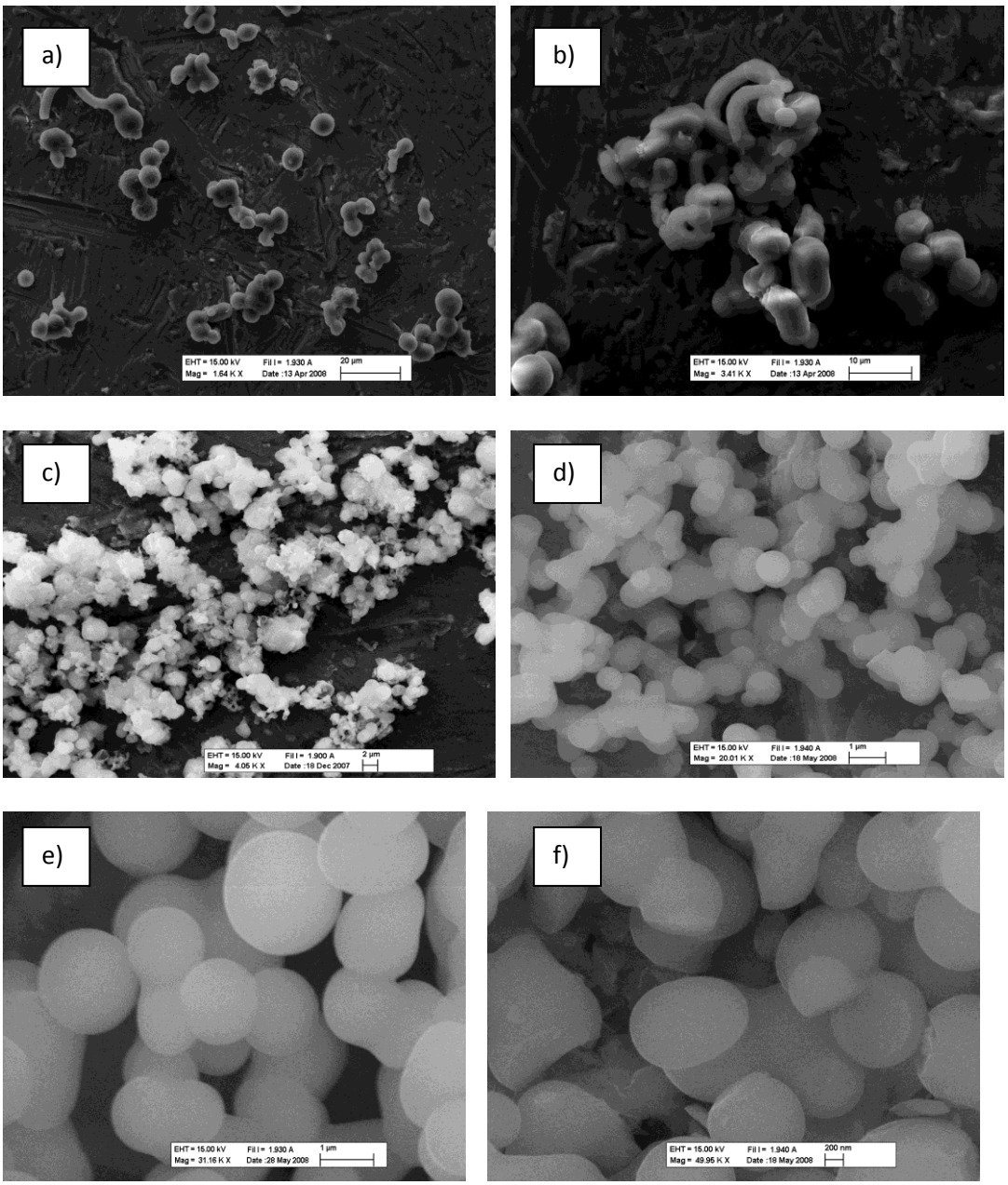

Figure 3.1.9: The SEM images of silica particles obtained from the SDS-P65 system with a SDS/P65 mole ratio of 3.0 and NaCl concentration of (a) 1.0M, (b) 0.50M, and (c) 0.25M.

3.2 Synthesis of Mesoporous Silica Using SDS-P123 Surfactant System

3.2.1 The Effect of SDS/P123 Mole Ratio to Mesoporous Silica Synthesis

The SDS/P123 mole ratio has been varied between 0 and 3 to investigate the effect of SDS/P123 mole ratio. In the absence of SDS, no silica particle or gel formation was observed even at high temperatures. Upon addition of SDS, first wormlike particles formed. At around 1 SDS/P123 mole ratio, a morphology change was observed from wormlike to a muffin shape, see Figure 3.2.1. When the SDS/P123 mole ratio reached to 2, mesoporous silica rods were formed. The silica rods have 10 μm diameter and 800-1000 μm length. When more SDS was added to the media, amorphous silica formation was observed. If the SDS/P123 mole ratio was increased above 2.5, the excess SDS formed mesostructured films at the air-water interface.

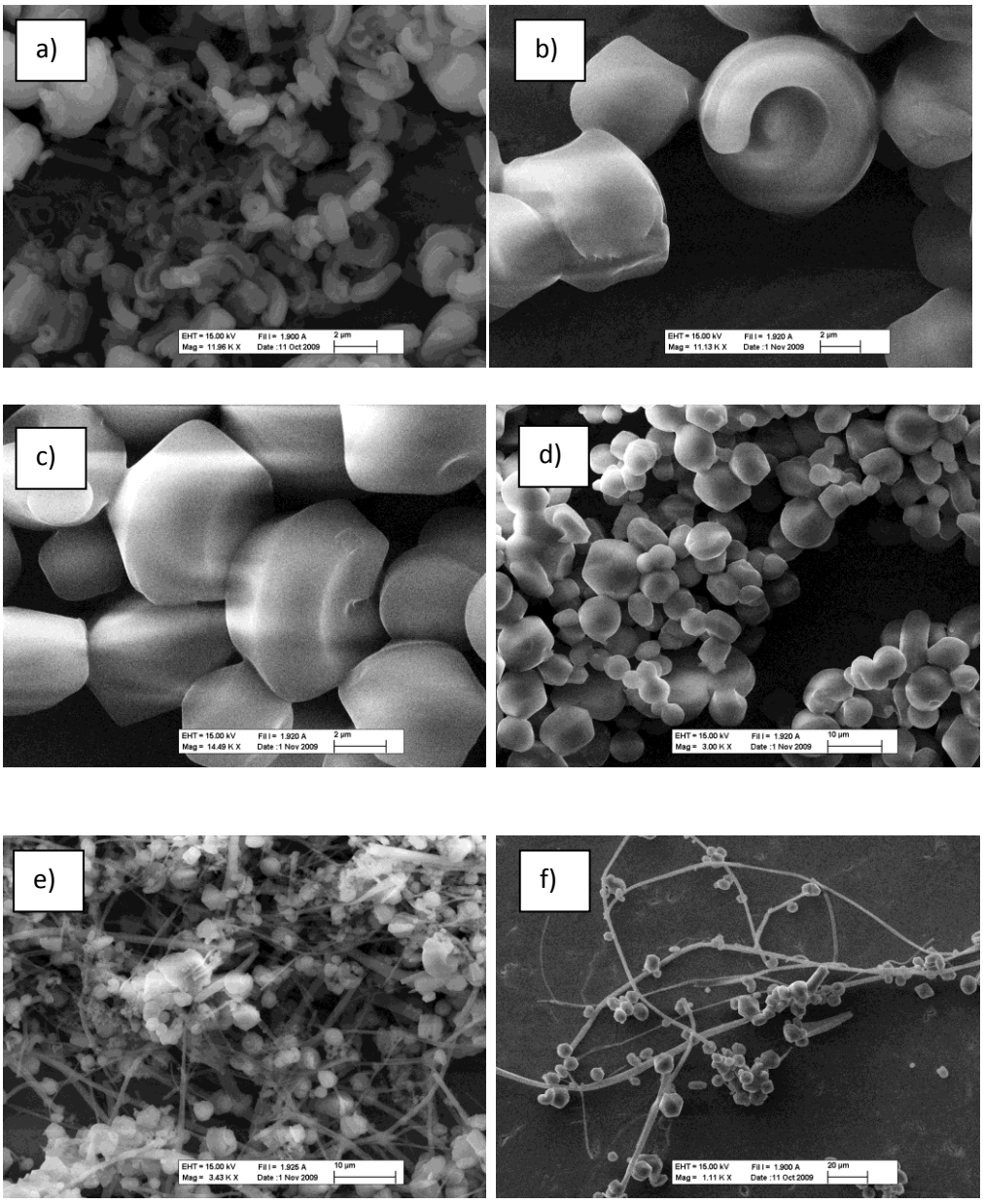

Figure 3.2.1: The SEM images of mesoporous silica particles obtained from the SDS-P123 system with a SDS/P123 mole ratio of (a) 0.25, (b)1.0, (c) 1.0, (d) 1.5, (e) 2.0, and (f) 2.0

The failure of mesoporous silica particle formation, in the absence of SDS, indicates the importance of negatively charged surfactant in the system. The negatively charged surfactant, controls the formed morphology formation, where the mole ratio of SDS to P123 determines the morphology. These observations overlap

well with the observations on the micellization of SDS and P123 in the literature. Ganguly and coworkers showed that the micelle shape is a function of SDS/P123 mole ratio, see Table 3.2.1 [59]. If there is no SDS, the aggregation number and the core radius of the P123 micelle are maximum. The core radius (Rc) and the hard-sphere radius (Rhs) gradually decrease with increasing SDS concentrations, on the other hand, the charged character of the micelle increases with increasing SDS concentration. The amount of SDS is very important to adjust both size and charge of the micelle, which are pivotal for the construction of mesostructures. Above 2.0 SDS/P123 mole ratios, the mixed surfactant micelle starts to disassemble. At 5.0 SDS/P123 ratios the aggregation number is lower than 4.0, which means SDS destroys the mixed micelles at high SDS concentrations. Above 2.0 SDS/P123 mole ratios, amorphous silica is formed. Therefore, the reduced aggregation number would be the reason for the loss of morphology. When the SDS/P123 mole ratio is over 2.5 film formation is observed at the air-water interface. The drastic decrease of the aggregation number of mixed micelles release free SDS molecules, which likely go to the water-air interface, form its own micelles and assemble with silica species to form the mesostructured film.

SDS conc. (mol/mol BC)	Core radius (R_c)(nm)	Aggregation number (N_{agg})	Hard-Sphere radius (R_{hs})(nm)	Volume fraction (Ø)	Polydispersity ΔRc/Rcm(%)	Shell Thickness (nm)
0	4.79	69	9.41	0.193	27	4.62
1:1	3.69	30	8.84	0.312	30	5.15
2:1	3.21	19	7.17	0.294	25	3.96
5:1	1.89	4	5.20	0.272	43	3.31

[Core Radius (*R*c), Hard-sphere Radius (*R*hs), Aggregation Number (*N*agg) (average number of surfactants per micelle), Volume Fraction (ø) (core to shell ratio), and Polydispersity (Δ*R*c/*R*cm)]

Table 3.2.1: The structural parameters of mixed micelles obtained from the SDS-P123 system with different SDS/P123 mole ratios [59].

To prove this, we also recorded the PXRD pattern of film samples, which display a diffraction lines at 2.42, 4.84 and 7.26, 2θ, (not shown) characteristic for mesoporous silica synthesized using SDS.

Up to 1.0 SDS/P123 mole ratio, the decrease in *R*c is considerably more than that in *R*hs, see Table 3.2.1. The difference between the *R*c and *R*hs represents the shell thickness and increases upon addition of SDS. This suggests that the PEO chains are stretched in the corona region of the micelles in the presence SDS ions. Notice that a morphologic transition is observed at a 1.0 SDS/P123 mole ratio from

wormlike particles to muffin shaped particles. The aggregation number of the surfactants and the core radius of the micelle decrease sharply causing an increase on the shell thickness, which gives rise to a significant increase in the volume fraction of the micelles, above this mole ratio. The observed increase in the micellar volume fraction is much larger than the contribution coming from the added SDS. This suggests that the degree of hydration of the micelles increases quite significantly in the presence of 1.0 SDS for each P123. Although the micellar volume fraction first increases upon addition of SDS, it decreases with a subsequent increase in the SDS concentration because of a decrease in the shell thickness. A higher rate of decrease of *R*hs as compared to that of *R*c leads to the observed decrease in the shell thickness. The triblock copolymer forms mixed micelles with SDS, and its aggregation number in the mixed micelles decreases with increasing SDS concentration. The volume fraction of the micelles, however, increases significantly in the presence of SDS because of an increase in the degree of hydration of the micelles in the corona region. It has been suggested that the increased hydration of the micelles is achieved by stretching of the EO blocks in the corona region in the presence of SDS molecules.

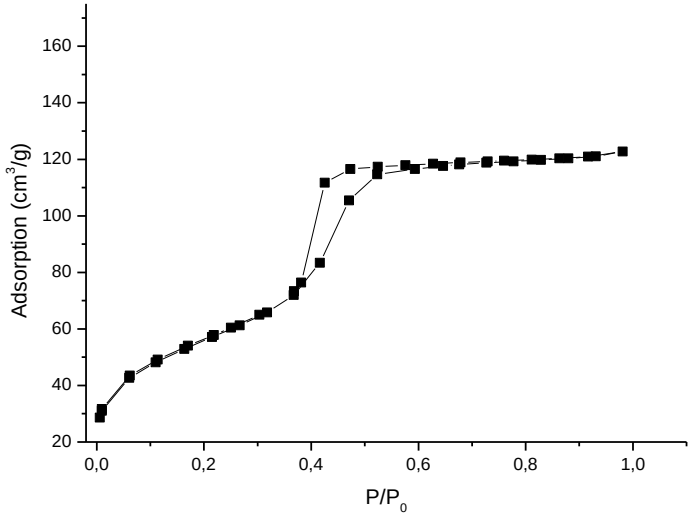

Figure 3.2.2: The N_2 adsorption-desorption isotherms of the silica particles at 77K obtained from the SDS-P123 system at 1.0 SDS/P123 mole ratio.

The N_2 adsorption-desorption isotherm of a sample prepared using 1.0 SDS/P123 mole ratio is shown in Figure 3.2.2. The isotherm is clearly type-IV, which is characteristic for mesoporous structures. The desorption branch of the isotherm generally gives information about the pore structure. The desorption branch generally shows hysteresis in the mesoporous structure because the capillary condensation causes late evaporation of N_2 from the pore surface. At the SDS/P123 mole ratio of 0,25 to 2.0, the desorption branch of the isotherm shows type-I hysteresis, which shows spherical, open and regular pores[78].

The BJH method was used to determine the pore diameter. Figure 3.2.3 shows narrow pore size distribution curve with an average pore diameter of 4.0 nm.

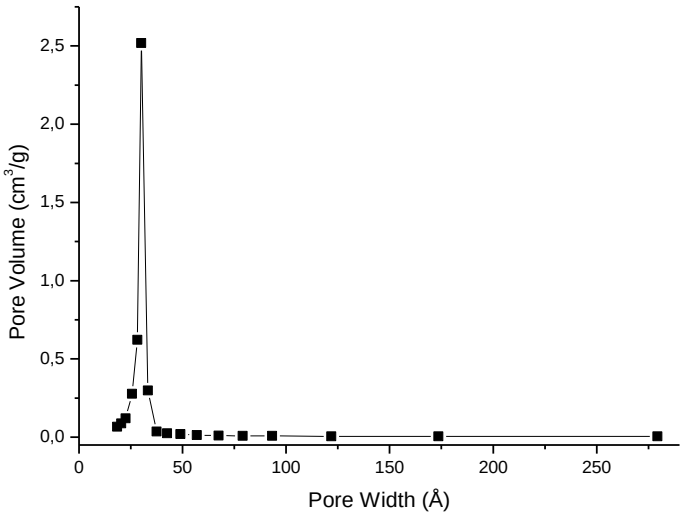

Figure 3.2.3: The BJH pore size distribution (diameter) of the particles obtained from the SDS-P123 system at a SDS/P123 mole ratio of 1.0.

The t-plot also indicates the pore structure in another manner. This method is used to determine existence of mesopores and micropores in the system. Figure 3.2.4 displays t-plot showing a downward deviation followed by upward deviation. This character of t-plot shows that there are two different pore structures (both micropores and mesopores) in the synthesized particles.

The BET data indicates that the synthesized particles have a total surface area of 450-650 m^2/g, in which 10-15% of the surface area is due to micropores. The small amount of microporosity is likely due to the covered hydrated ethylene oxide groups of pluronic surfactants with silica species.

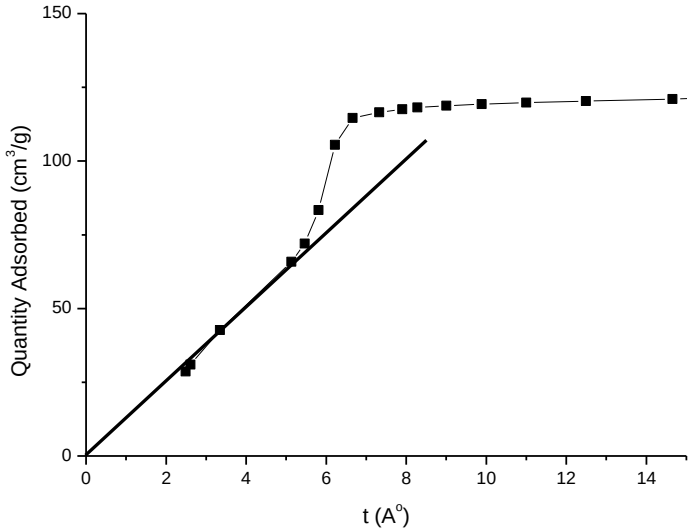

Figure 3.2.4: The t-plots for N_2 adsorption isotherms of the silica particles obtained from the SDS-P123 system at a SDS/P123 mole ratio of 1.0 at 77K.

The structural details of the silica particles synthesized using the SDS-P123 couple was investigated using the PXRD technique. The silica synthesized using only neutral tri-block co-polymer, P123, in the media, has disordered structure and does not diffract at small angles (Figure 3.2.5). Increasing SDS/P123 mole ratio from 0.5 to 1.0, increases the order of the structures with a 2D-Hexagonal structure where the unit cell parameter, a, shifts from 7.7 nm to 8.0 nm. Table 3.2.1 shows increasing volume fraction at the same ratio and correlates with increasing unit cell parameter. Going from1.0 to 2.0 SDS/P123 mole ratio, the unit cell parameter regress to 7.7 nm from 8.0 nm. The decrease on the unit cell parameter is again related with the decrease of the volume fractions of the micelle by shrinkage of the shell thickness at that ratio.

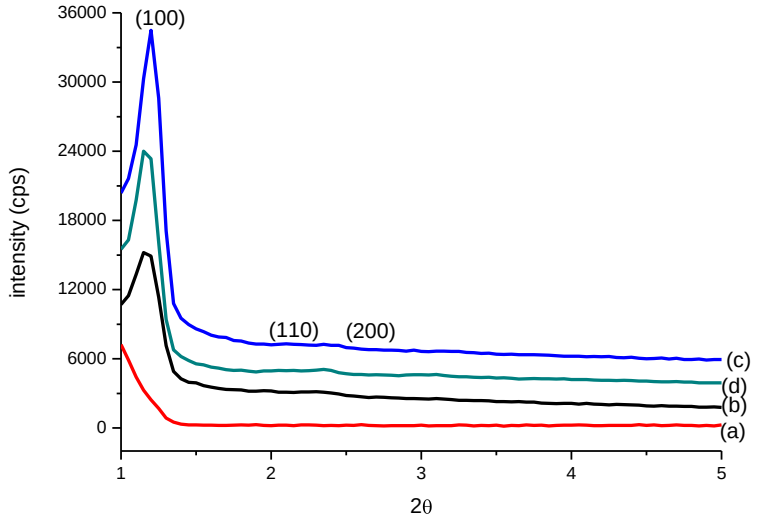

Figure 3.2.5: The PXRD patterns of the mesoporous silica particles obtained from SDS-P123 system at SDS/P123 mole ratio of (a) 0.0, (b) 0.25, (c) 0.75, and (d) 1,75.

Table 3.2.2 contains the values of the wall thickness, pore size, repeating unit and the pore volume of the synthesized particles with increasing SDS/P123 mole ratios. The information in Table 3.2.1 correlates well with the data in Table 3.2.2. The trends of the shell thickness of the micelle can be seen in the wall thickness measurements of the synthesized samples. The pore radii of the samples are very similar with the core radius of the micelles, mentioned in the Table 3.2.1. Also the repeating units of the samples have close values with the hard sphere radius of the micelles. The strong correlation between Table 3.2.1 and Table 3.2.2 indicates again that the control of the mixed micellar system plays significant roles on the mesostructure of the mesoporous silica particles. However, there is no relation between the surface area of the samples and the SDS/P123 mole ratios. The surface area changes in the range between 460 and 630 m^2/g and the pore sizes in the

intervals between 3.2 nm and 4.1 nm. The pore volumes of the synthesized samples were around 0.50 cm^3/g, which also indicates that samples are mesoporous.

SDS-P123 mole ratio	Surface Area[a] (m^2/g)	Repeating unit (Å)[b]	Pore size (Å)[c]	Pore Volume (cm^3/g)[d]	Wall thickness (Å)[e]
2.00	542	77	32	0.43	45
1.75	523	77	36	0.42	39
1.50	541	77	33	0.44	44
1.25	520	80	34	0.45	46
1.00	466	80	33	0.39	47
0.75	542	73	33	0.45	40
0.50	610	77	39	0.50	38
0.25	632	85	41	0.52	44

a: BET surface area, b:a parameter ($a=d\sqrt{3}/2$), c: BJH desorption pore size distribution

d:BET pore volume, e: wall thickness = a parameter – BJH pore size distribution

Table 3.2.2: The structural parameters of the mesoporous silica obtained from the SDS-P123 system.

The particles were further characterized, using TEM and POM. The TEM images of the silica particles are shown in Figure 3.2.6. The pores on the surface can be seen easily. The pores are ordered and they have pore diameter of about 4.0 nm. This pore size obtained from TEM correlates with the data, obtained using both N_2 adsorption-desorption method and the PXRD techniques. The BJH desorption curve shows narrow pore size distribution with 30-40 angstroms pores. The PXRD data gives the unit cell parameter as 7.7 nm, which is also observed in the TEM images.

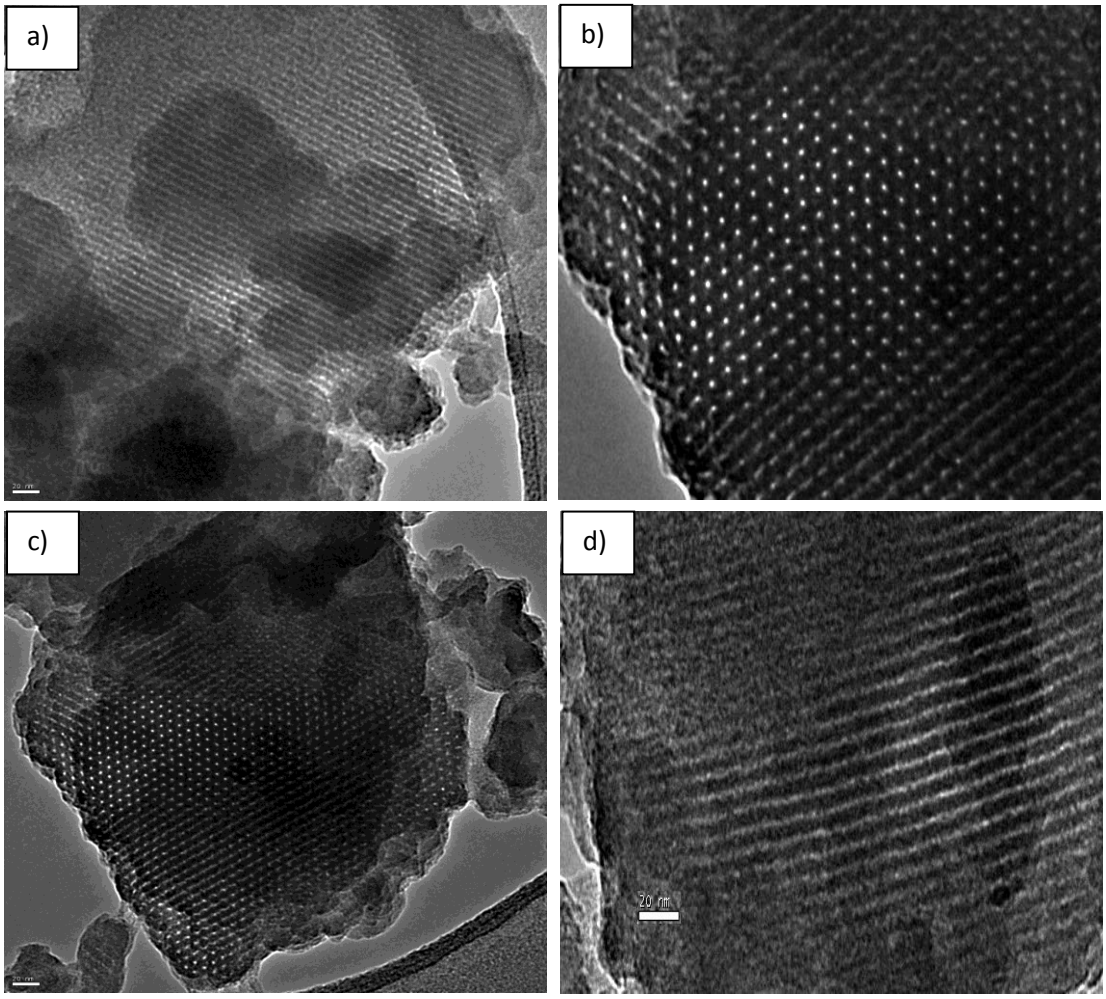

Figure 3.2.6: The TEM images of the particles obtained from the SDS-P123 system at 2.0 SDS/P123 mole ratio.

The polarized optical microscopy images of the silica particles are shown in Figure 3.2.7. Between the cross polars the particles are birefringent, which means that the synthesized silica particles are anisotropic. The silica particles are ordered and have a 2D-hexagonal structures. Note that birefringence exists only if the structure of the material is anisotropic (directionally dependent). The maltese crosses observed at higher magnifications, Figure 3.2.7 (d), is characteristic for the 2D-hexagonal mesostructures.

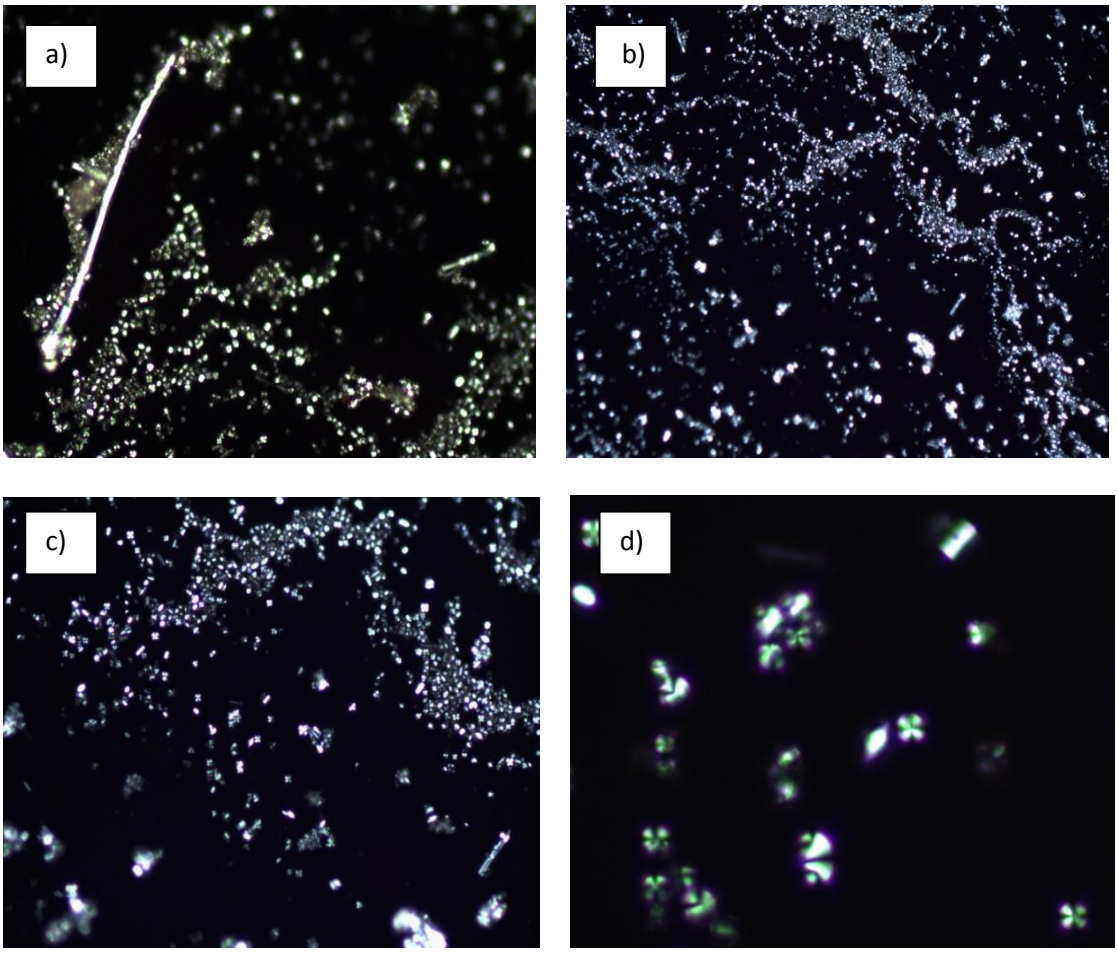

Figure 3.2.7: The POM images of the mesoporous silica particles obtained from the SDS-P123 system at a SDS/P123 mole ratio of 2.0 recorded from different part of the samples or magnifications.

Figure 3.2.8 shows the optical microscopy images of the rods obtained from the SDS-P123 system at 19^0C. The rods are approximately 10 μm wide and up to 1000 μm long. At the special conditions, the rod morphology is dominant morphology.

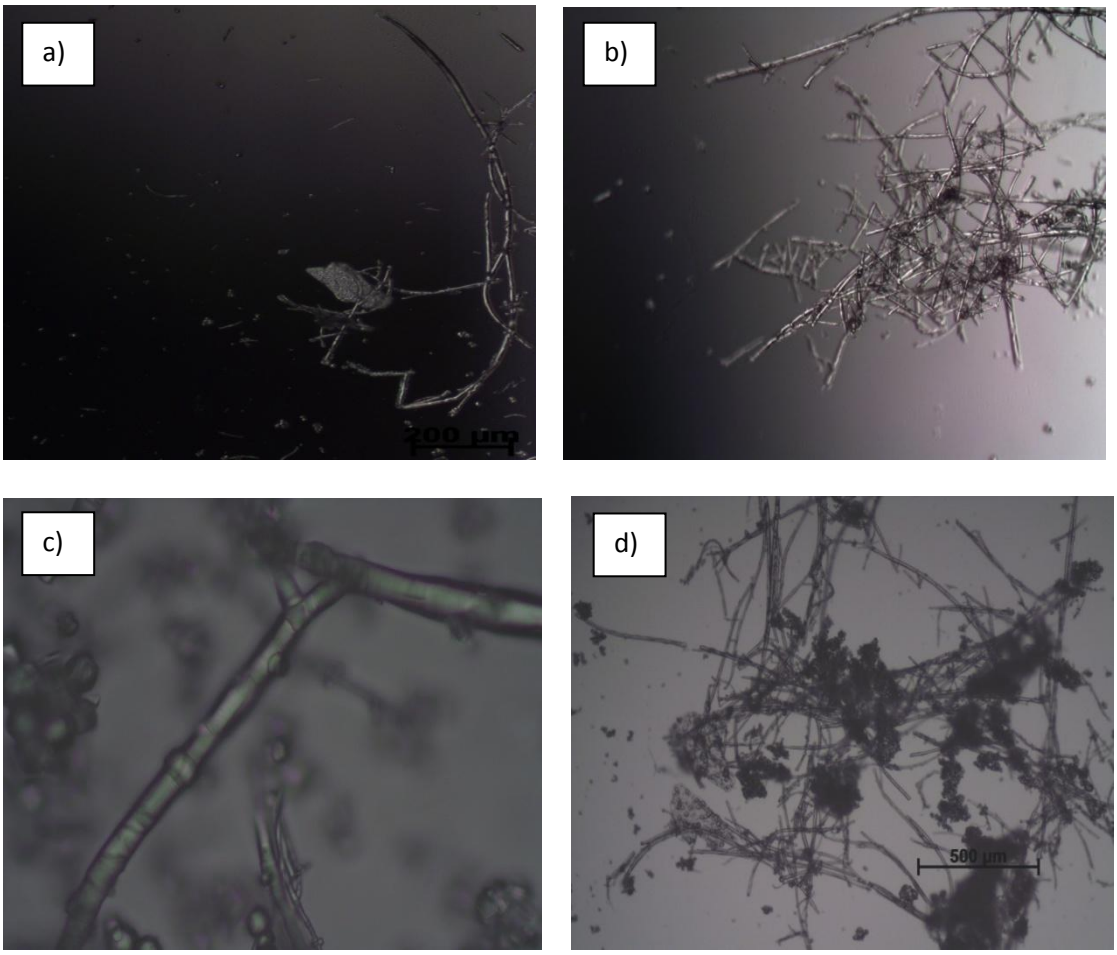

Figure 3.2.8: The regular optical microscopy images of the mesoporous silica particles obtained from the SDS-P123 surfactant system at a SDS/P123 mole ratio of 2.0, recorded from different parts of the sample or magnifications.

3.2.2 The Effect of Synthesis Temperature to the SDS-P123 Surfactant Systems

The temperature of the reaction media is also important for synthesizing mesoporous silica particles in the SDS-P123 surfactant system. To understand the effect of temperature on morphology and formation of silica particles a series of experiments have been designed in a temperature range of 15 to 35^0C. To investigate

the effect of temperature, independently from pH and SDS/P123 mole ratio, fixed and optimized conditions for the pH and SDS/P123 ratio have been used. The SDS/P123 mole ratio was set to 2.0 and pH was set to 1.0. The experiments have been carried at 35, 30, 27, 25, 23, 21, 19, 17 and 15^0C and it has been shown that over 27^0C, a gel formation occurs. This gel formation results in disordered amorphous silica particles. The reaction is a temperature dependent process and shortens with increasing temperature. This enabled us to control morphology, size and meso-order of the silica particles by controlling the reaction temperasture. Figure 3.2.9 shows morphologic changes with temperature. The silica rod formation is observed when the temperature is 21^0C. The rods have 1000 μm length and 10-15 μm diameter. The sphere like morphologies are also observed together with those rods. However, the rods are the dominant particles. When the temperature is decreased to 19^0C, no rod formation is observed, instead small individual particles have been obtained with approximately 10-20 μm length and 10-15 μm width. However, when the temperature was decreased to 17^0C, the individual particles cannot be formed. Aggregated curly fibers are observed at17^0C.

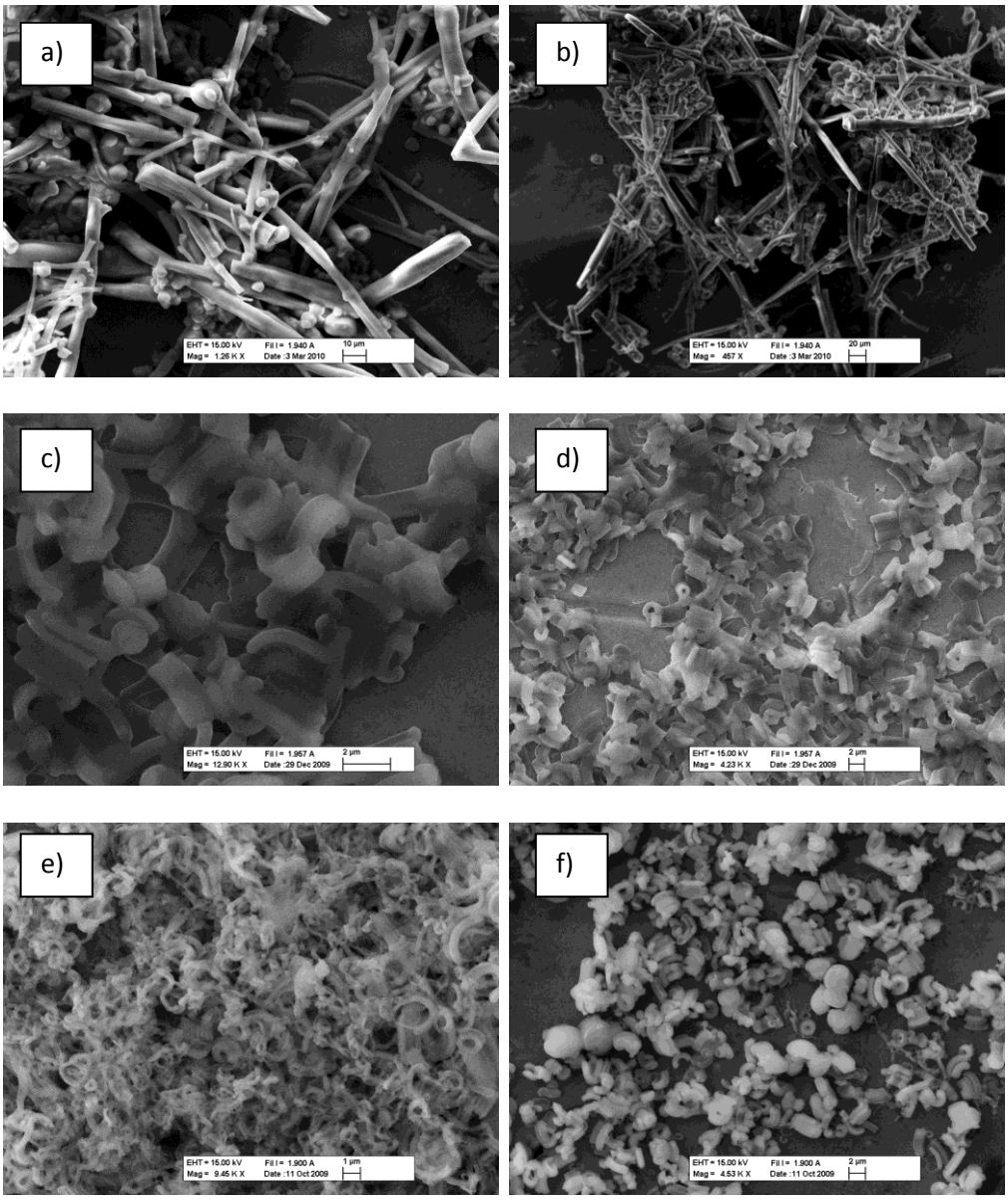

Figure 3.2.9: The SEM images of mesoporous silica particles obtained from the SDS-P123 system with a SDS/P123 mole ratio of 2, at pH 1.0 and the temperature of a, b) 21^0C, c, d)19 ^{0}C, and e, f)17 ^{0}C.

The synthesized particles at different reaction temperatures were further investigated using PXRD technique. Figure 3.2.10 shows the diffraction patterns of the samples synthesized at different temperatures. The PXRD investigation showed that the diffraction line intensity is maximum at 19^0C, the meso-order decreases at

21^0C and at 17^0C. The PXRD data shows that the all the samples are meso-ordered and the unit cell parameter "a" is temperature dependent. Figure 3.2.10 clearly shows that the meso-order increases with increasing temperature up to 19^0C. The Peak at 1.14, 2θ is due to (100) planes of the 2D hexagonal structure. The broad feature between 1.9 and 2.8 , 2θ is due to (110) and (200) planes. This corresponds to a unit cell parameter 'a' of 77 Å.

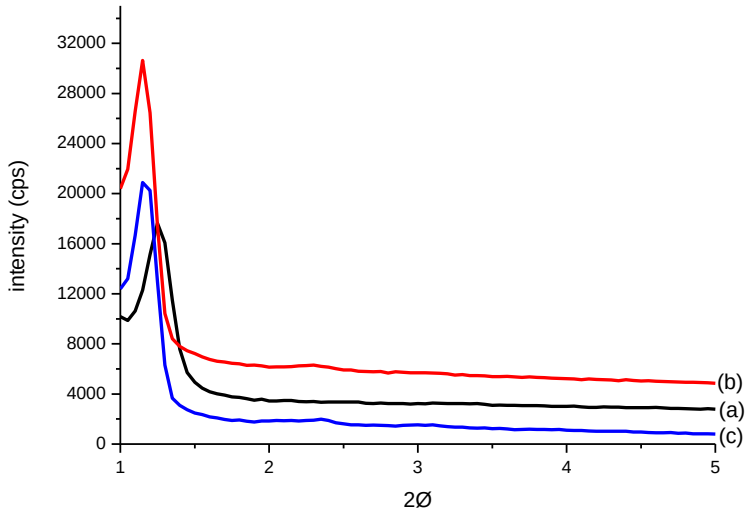

Figure 3.2.10: The PXRD patterns of the mesoporous silica particles obtained from SDS-P123 system at temperatures of a) 17 ^{0}C, b)19 ^{0}C, and c) 21^0C.

To understand the pore structure and the surface properties of the silica particles, synthesized at different temperatures, the N_2 adsorption-desorption isotherms were also recorded. All the samples synthesized in the temperature range of 17 and 23^0C have characteristic type-IV isotherms, indicating that the particles are mesoporous, see Figure 3.2.11. The desorption branch generally shows hysteresis in the mesoporous structure, because the capillary condensation causes late evaporation of

N_2 from the pore surface. Between the temperatures 17 to 23^{0}C, the desorption branch of the isotherm shows type-I hysteresis, showing that the pores are spherical, open and regular.

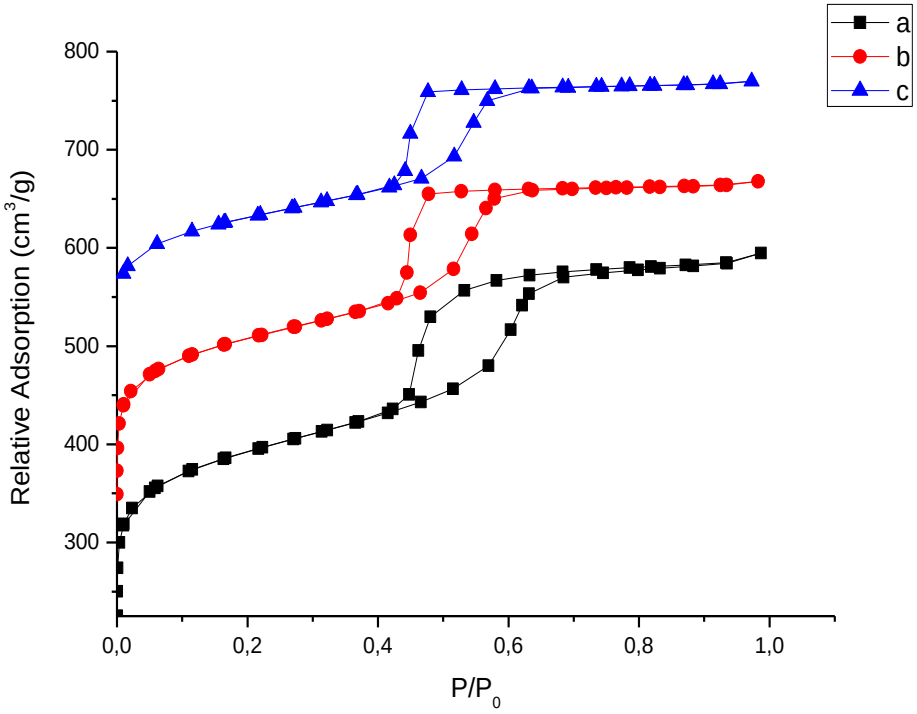

Figure 3.2.11: The N_2 adsorption-desorption isotherms, at 77K, of the mesoporous silica particles obtained from the SDS-P123 system at a) 17 ^{0}C, b)19 ^{0}C, and c) 21^{0}C.

To understand the pore diameter and pore size distribution, the BJH method was employed to desorption isotherm. The pore size distribution is very narrow and the average pore diameter is about 4.0-4.5 nm, see Figure 3.2.12. The pore diameters of the synthesized silica particles were independent from the synthesis temperature.

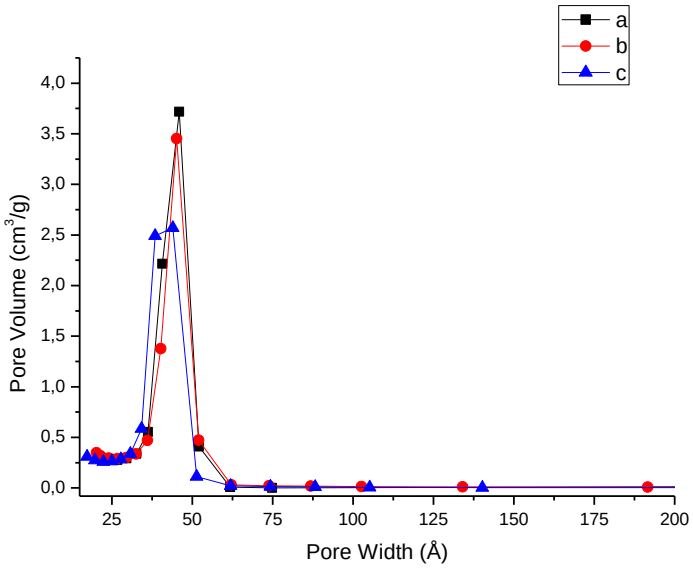

Figure 3.2.12: The BJH pore size distribution (diameter) for the mesoporous silica particles obtained from SDS/P123 system at the temperatures of a) 17 ^{0}C, b)19 ^{0}C, and c) 21^{0}C.

The t-plot is also very helpful to determine the existing pore types of the synthesized silica particles, synthesized at different temperatures using SDS-P123 system. Because of the upward and downward deviations from the linearity of the t-plots indicates micro and meso porosity of the samples 21^{0}C. At the synthesis temperatures 17 and 19^{0}C t-plots have only upward deviations from linearity, indicating that the structures have only mesopores.

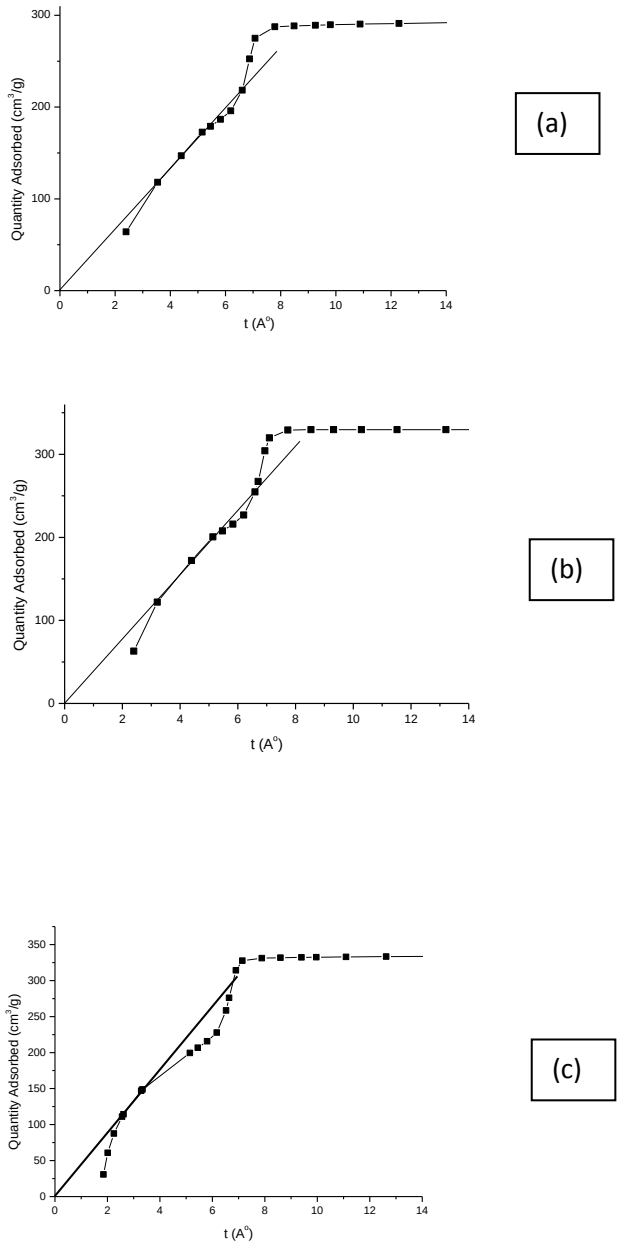

Figure 3.2.13: The t-plots of the N_2 adsorption isotherms at 77 K for the mesoporous silica particles synthesized at a) 17 ^{0}C, b) 19 ^{0}C, and c) 21^{0}C.

Under the light of the data obtained from PXRD patterns, N_2 adsorption-desorption isotherms and images obtained from SEM, it could be concluded that, the synthesis temperature is highly effective on the morphology and pore structure of the mesoporous silica particles. The temperature interval, between 17 and 23^{0}C, has been found ideal for the mesoporous silica particle synthesis using SDS and P123 as the

templates. The detailed investigations, in this optimized temperature intervals have indicated that changing temperature plays a role on the morphology of the silica particles, Figure 3.2.9. The N_2 adsorption desorption technique indicated that there is no drastic change in the total surface areas but the pore structure of the samples changed when temperature is increased from 19 to 21^0C. Up to 19^0C there are no micropores in the structures however above this point small amount of micropores has been observed together with mesopores.

3.2.3 The Effect of Chloride Ion in the Synthesis of Mesoporous Silica

The effect of KCl to the SDS-P123 system was investigated by using different amounts of KCl at pH 1.0, 19^0C and a SDS/P123 mole ratio of 2.0. KCl was added to the reaction media at 0.1M, 0.25M, 0.50M, 0.75M and 1.0M concentrations. It is known that the chloride ion has an effect on both micellization of the surfactants and the polymerization of the silica species in an aqueous media [34, 47, 61, 75-77]. We have also investigated the effect of Cl^- on the SDS-P65 system where the Cl^- ion has a positive effect on the micellization and silica polymerization. Figure 3.2.14 shows the effects of Cl^- ion on the morphology. Increasing the amount of chloride ion changed the muffin shaped morphology to the less ordered morphologies. The identical particles aggregate together to form more complex morphologies at higher salt contents.

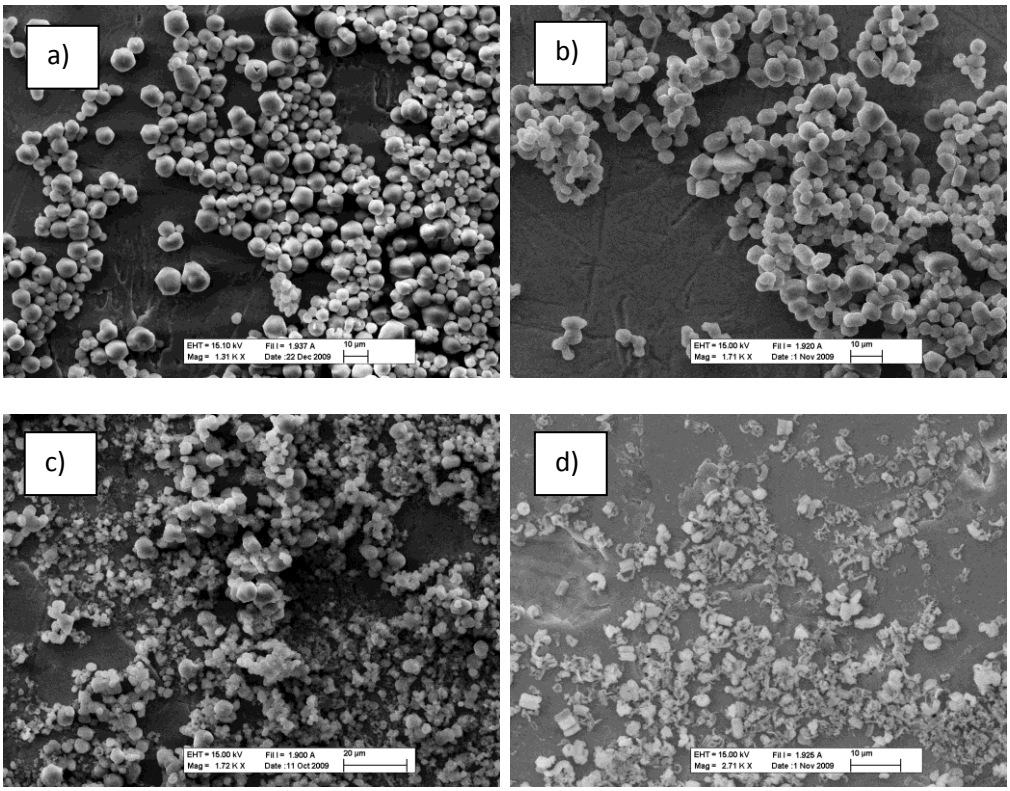

Figure 3.2.14: The SEM images of the silica particles obtained from the SDS-P123 system at 19^0C with KCl concentrations of (a) 0.25M, (b) 0.50M, (c) 0.75M, and (d) 1.0M

The PXRD patterns of the synthesized silica particles in the presence of the Cl^-, display an intense diffraction line at 1.2^o, 2θ. Its intensity increases with increasing concentration of chloride ion up to 0.5M. Further increment of the Cl^- ion concentration to 1.0M decreases intensity of this line, see Figure 3.2.15. The unit cell parameter "a" of the synthesized samples in the presence of different amounts of Cl^- are very close to each other. The diffraction line observed at 1.2^o, 2θ are due to (100) planes of 2D-Hexagonal mesostructure with a unit cell parameters of 7.2 nm. The broad features at 1.8 and 3.1^o , 2θ is due to (110) and (200) planes, respectively, of the 2D-Hexagonal mesostructure.

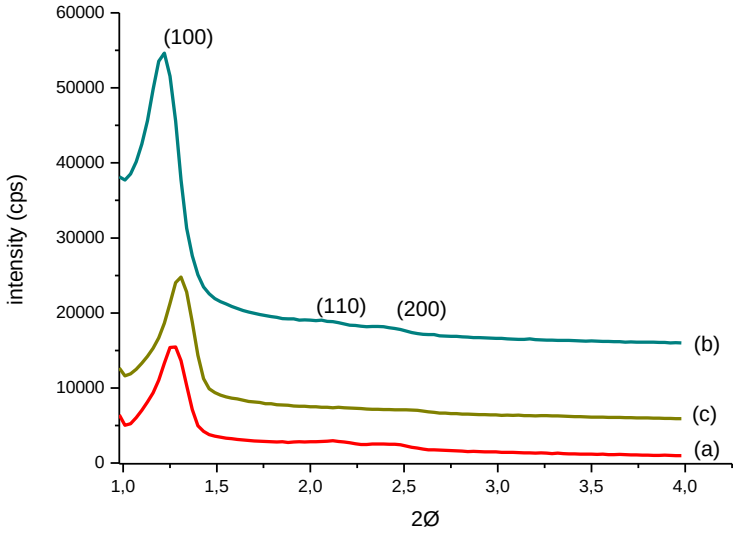

Figure 3.2.15: The PXRD patterns of the mesoporous silica particles obtained from the SDS-P123 system at 19^0C with KCl concentrations of (a) 0.25M, (b) 0.50M, and (c) 1.0M.

The N_2 adsorption-desorption isotherms have indicated that the synthesized particles, in the presence of different concentrations of KCl are mesoporous, see Figure 3.2.16. The N_2 sorption curves display type-IV isotherms, which are characteristic for mesoporous structures. The desorption branch of all isotherms have type-I hysteresis caused by capillary condensation. The type-I hysteresis is an indication for open, regular and spherical mesopores [53, 78].

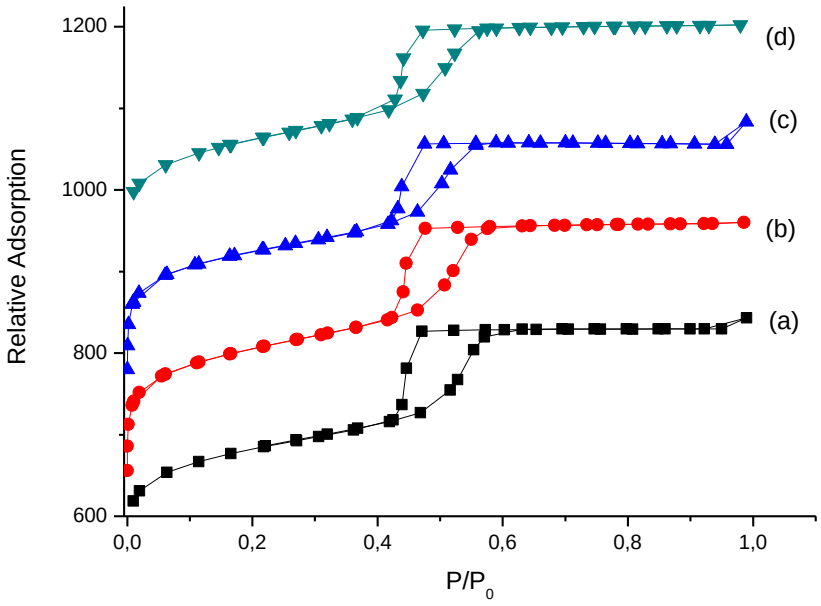

Figure 3.2.16: The N_2 adsorption-desorption isotherms at 77K for mesoporous silica particles obtained from the SDS-P123 system at 19^0C with KCl concentrations of (a) 0.25M, (b) 0.50M, (c) 0.75M, and (d) 1.0M

The BJH desorption curves show that the pore diameters of the synthesized silica particles are slightly changing with an increasing chloride ion concentration (Figure 3.2.17). The pore diameter increases from 4.0 nm to 6.0 nm, when the KCl concentration is decreased from 1.0M to 0.25M, see Figure 3.2.17. The pore size distribution of the synthesized silica particles are very narrow. The t-plots display characteristic downward deviation, continuing with upward deviation indicating the presence of mesopores together with micropores, see Figure 3.2.18.

Morphology of the particles can be controled by using ideal amount of KCl in the SDS-P123 system at optimum pH and temperatures. The meso-order is also a function of CI^- concentration. Both diffraction intensity and narrower pore size distribution in the BJH desorption curves indicate increasing meso-order in the

samples due to presence of Cl^- ion in the synthesis media up to chloride ion concentration is 0.5 M.

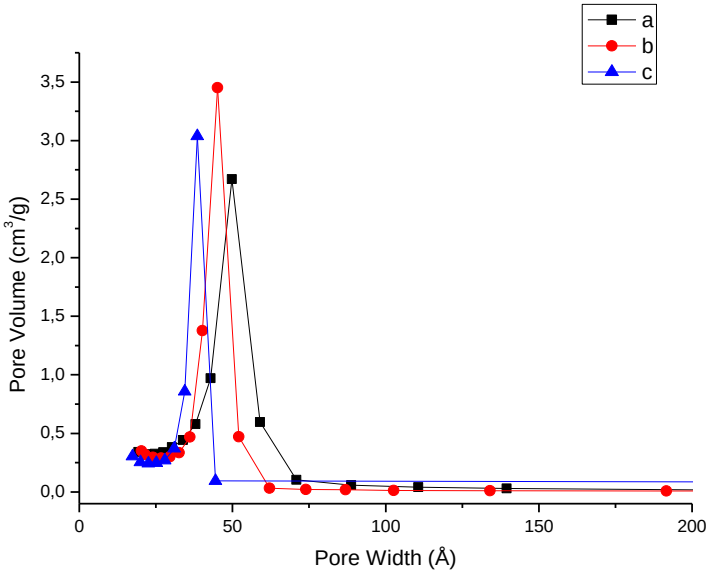

Figure 3.2.17: The BJH pore size distribution (obtained from desorption branch) of the mesoporous silica particles obtained from the SDS-P123 system at 19^0C and KCl concentrations of (a) 0.25M (5.0 nm), (b) 0.50M (4.5 nm), and (c) 1.0M (3.7 nm)

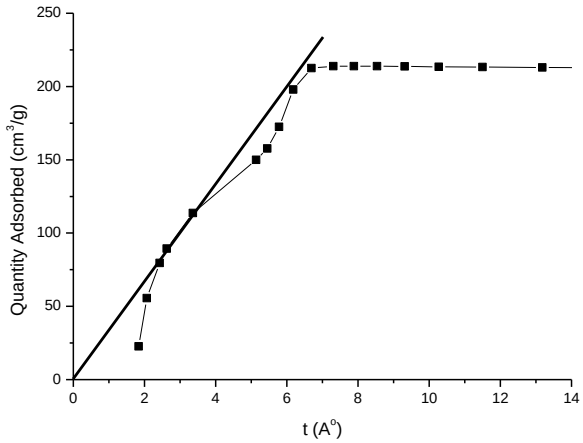

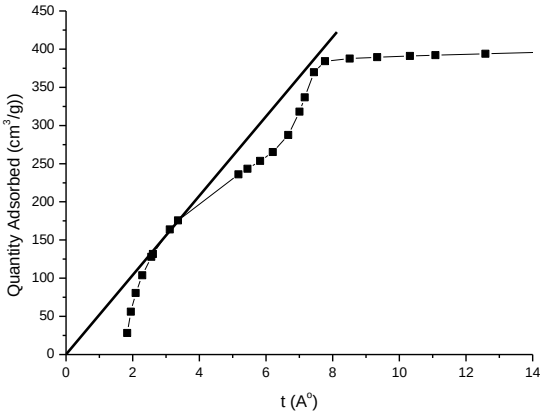

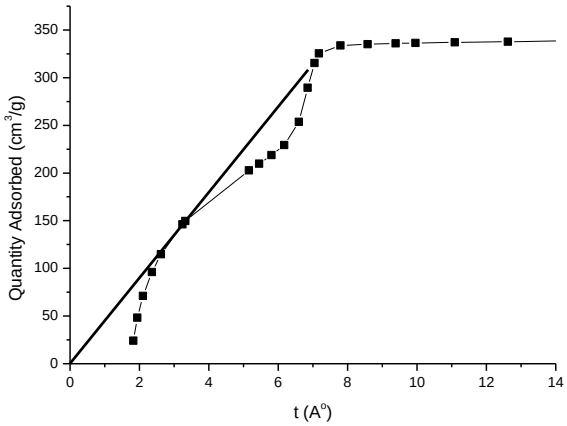

Figure 3.2.18: The t-plots, obtained from the N_2 adsorption isotherms (at 77K) of the mesoporous silica particles obtained from the SDS-P123 system at 19^0C and KCl concentrations of (a) 0.25M, (b) 0.50M, and (c) 1.0M

3.2.4 The Effect of TMOS Amount on the Mesoporous Silica Synthesis in the SDS-P123 system

Another important factor that determines the morphology and meso-structure of the synthesized silica particles is the amount of the silica source, TMOS (tetramethylorthosilicate). The TMOS amount is a very critical parameter to obtain well defined morphology with mesoporocity. Using TMOS in slightly deficient amounts results in silica particles with undefined morphologies. However, if the TMOS amount is used in an excess amount, it results in particles with plugged pores and disordered particles. By changing this parameter carefully, pore size can be adjusted.

At an optimized condition such as, 19^0C, pH of 1.0 and SDS/P123 mole ratio of 2.0; the TMOS amount was doubled and the structures of these two samples were investigated using SEM, PXRD and N_2 adsorption-desorption techniques. Figure 3.2.19 shows the SEM images of the synthesized silica particles, obtained using two different TMOS amounts. The particles obtained using 1.0g TMOS have a unique morphology with a 10 μm diameter and almost monodisperse. However, when the TMOS amount is doubled, 2.0g, the excess silica covered the particles.

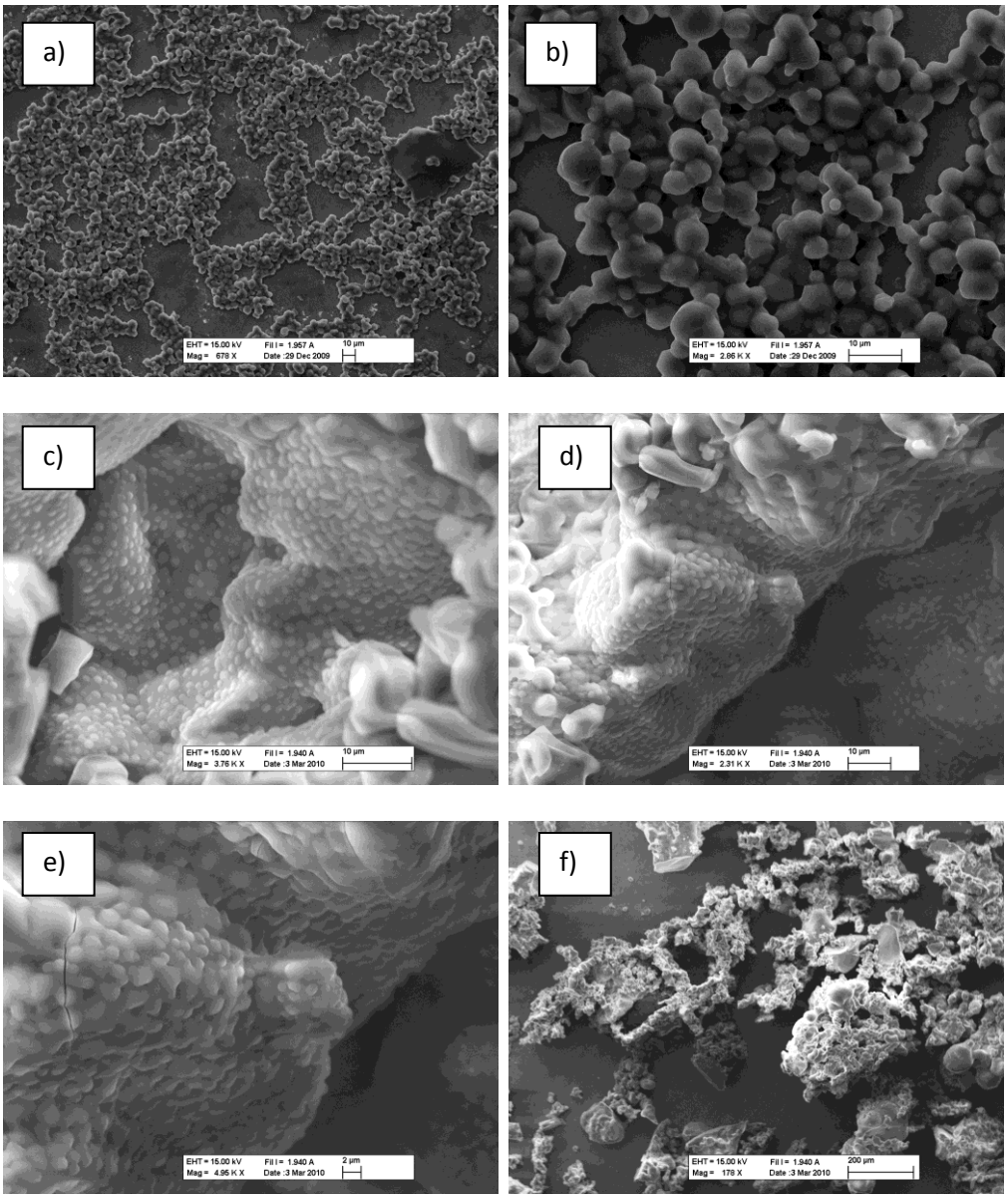

Figure 3.2.19: The SEM images of mesoporous silica particles obtained from the SDS-P123 system with TMOS amount of (a, b) 1.0g, (c, d) 2.0g, and (e, f) 2.0g. Images were recorded from different part of the samples.

Figure 3.2.20 shows the PXRD patterns of the silica particles, synthesized using 1.0g and 2.0 g of TMOS. The excess TMOS shifted the unit cell parameter "a" to a smaller value. The peak at 1.20^0, 2θ shifted to 2.32^0, 2θ. Moreover the intensities of the two peaks are almost same.

The Peak at 1.2^0, 2θ is due to (100) plane and the broad features between 1.8 and 3.2^0, 2θ is due to (110) and (200) planes of the 2D hexagonal structure with a unit cell dimension of 73 nm, Figure 3.2.20(a). However the only line observed at 2.32^0 in the samples prepared using 2.0g of TMOS could be due to (100) or (110) planes of the same structure. It is difficult to make a clear determination of the structure using only PXRD data . Therefore, the N_2 adsorption-desorption isotherms are need to resolve this controversy.

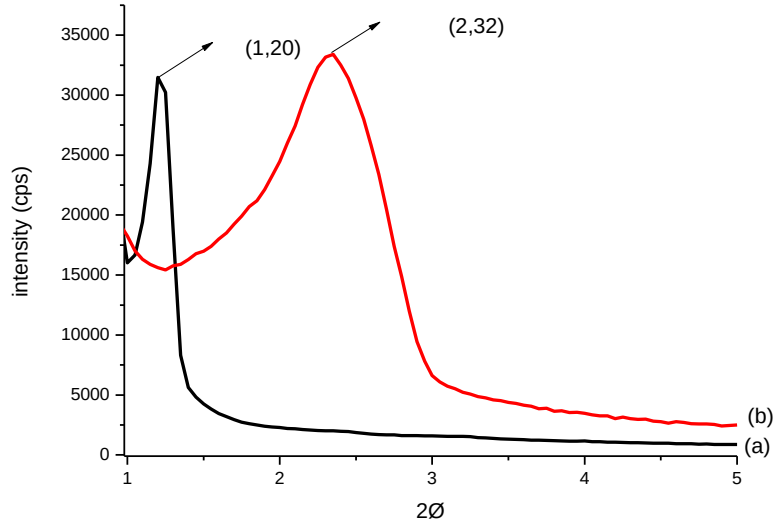

Figure 3.2.20: The PXRD patterns of mesoporous silica particles obtained from the SDS-P123 system with the amounts of TMOS in 100 ml solution (a) 1.0g, and (b) 2.0g.

The N_2 adsorption desorption branches of the silica samples synthesized using different amounts of TMOS show type-IV isotherms characteristics for mesoporous silica. In the desorption branch of the isotherms, the type-I hysteris can be seen, resulting from the capillary condensation. The silica particles synthesized in the presence of excess TMOS showed a smaller hysteresis branch that can be interpreted

as a shrinked pore diameter. Because of a smaller pore size, capillary condensation of the N_2 molecules in the pores is much lower, which leads smaller hysteris path in the desorption branch of the isotherm.

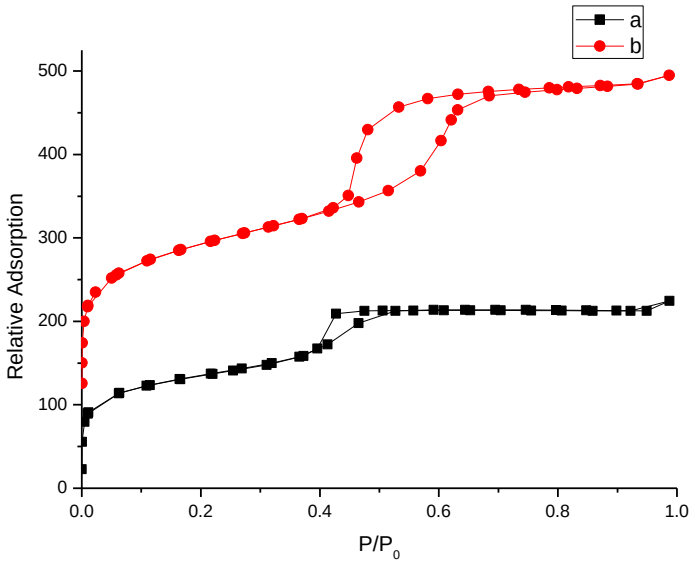

Figure 3.2.21: The N_2 adsorption-desorption isotherms (at 77K) of the mesoporous silica particles obtained from the SDS-P123 system using TMOS amount of (a) 1.0g, and (b) 2.0g.

The pore size distribution of the synthesized silica particles obtained from different amount of TMOS were also investigated using BJH method using the desorption branch of the isotherms. Increasing the amount of TMOS causes shrinkage in the pore diameter, which correlates with the PXRD data, Figure 3.2.22. The pore size distribution also shows that the pore diameter shrinks from 5.0 nm to 3.3 nm, upon doubling the amount of TMOS in the synthesis media.

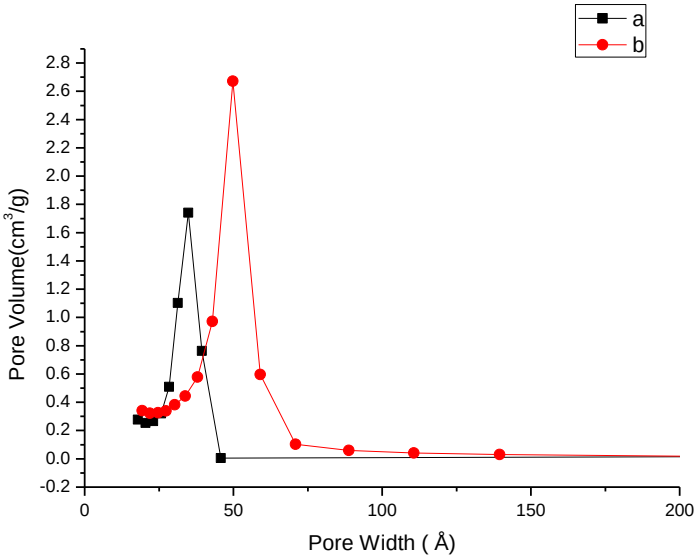

Figure 3.2.22: The BJH pore size distribution (using desorption branch) of the mesoporous silica particles obtained from the SDS-P123 system using TMOS amounts of (a)1.0g (3.5nm), and (b) 2.0g(5.0).

The t-plots show downward deviation first and then continuing with upward deviation from the linearity, see Figure 3.2.23, indicating existence of both micro and mesopores. Moreover, the silica particles synthesized in the presence of excess TMOS have macropores, which can be seen in the SEM images.

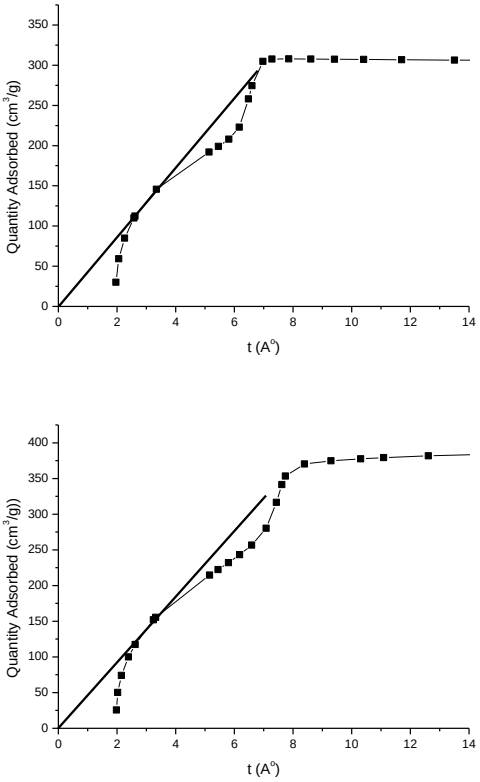

Figure 3.2.23: The t-plots for N_2 adsorption isotherms (at 77K) of the mesoporous silica particles obtained from the SDS-P123 system using TMOS amount of (a) 1.0 g, and (b) 2.0 g.

3.2.5 The Effect of Nitrate Ion on the Synthesis of Mesoporous Silica in the SDS-P123 System

The nitrate anion effect has also been investigated in the SDS/P123 mixed surfactant system by using different amounts of $NaNO_3$ in the synthesis media. The effects of $NaNO_3$ has been investigated at concentrations of 0.1, 0.25, 0.50, 0.75, and 1.0M at 19^0C, pH of 1.0 and the SDS/P123 mole ratio of 2.0. The nitrate ion has a definite effect on the morphology, see Figure 3.2.24. When the 0.25M $NaNO_3$ was used, the identical particles aggregate together to form bulky particles. When more nitrate ion

is added, such as 0.50M, a well defined morphology apperars again, a distorted sphere and distorted muffin shaped silica particles with particle size of about 5.0 μm. When the nitrate ion concentration is increased to 0.75M, a partially aggregated wormlike morphology has been observed. The worm like silica particles, have 6.0 μm diameter and 15-20 μm length. At this concentration small amount of silica spheres were also observed together with wormlike particles. When the nitrate ion concentration increases to 1.0M, the rod or fiber morphology has been formed. The synthesized silica rods have 8-10 μm diameter and 200-400 μm length. It is obvious that the slight change of the nitrate ion concentration drastically changes the silica particle morphology in the SDS-P123 surfactant system.

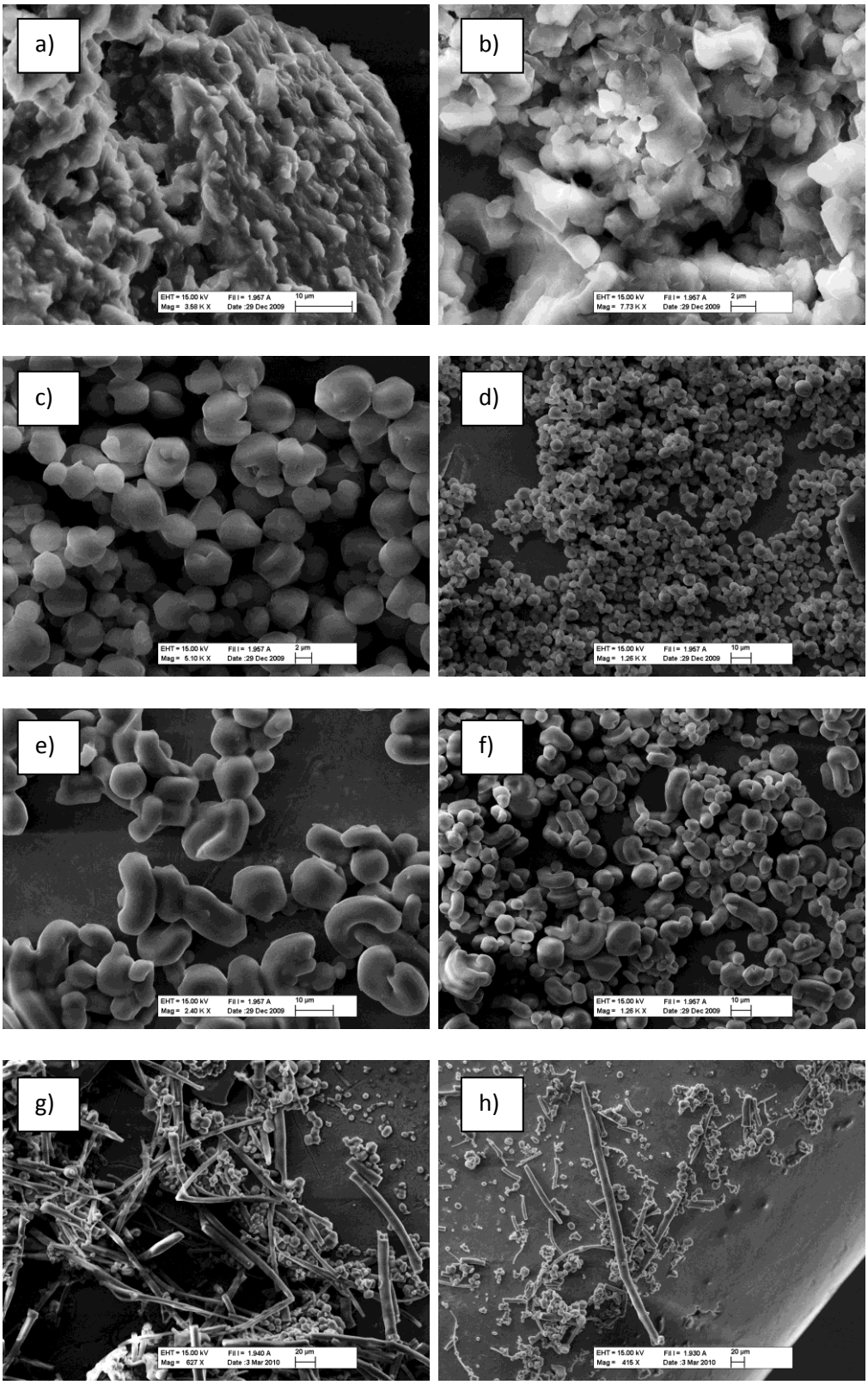

Figure 3.2.24 The SEM images of the silica particles obtained from the SDS-P123 system at 19^0C with $NaNO_3$ concentrations of (a) 0.25M, (b) 0.25M, (c) 0.50M, (d) 0.50M, (e) 0.75M, (f) 0.75M, (g) 1.0M, and (h) 1.0M

The PXRD patterns of the synthesized silica particles in the presence of different nitrate ion concentrations are shown in Figure 3.2.25. The increasing nitrate ion concentration in the synthesis media shifted the diffraction line of the particles to higher angles, see Figure 3.2.25. The unit cell parameter "a" drops from 7.3 nm to 4.6 nm with an increasing NO^{-}_{3} concentration in the reaction media. The peak at 1.20^{0}, 2θ is due to (100) planes of the 2D hexagonal structure. The broad feature between 1.8 and 3.0^{0}, 2Ø is due to (110) and (200) planes. This corresponds to a unit cell dimension of 7.3 nm, see Figure 3.2.25(a). The peaks at 1.82 and 1.90^{0}, 2θ are due to (100) planes of the 2D hexagonal structures of the silica particles, obtained at higher nitrate ion concentrations.

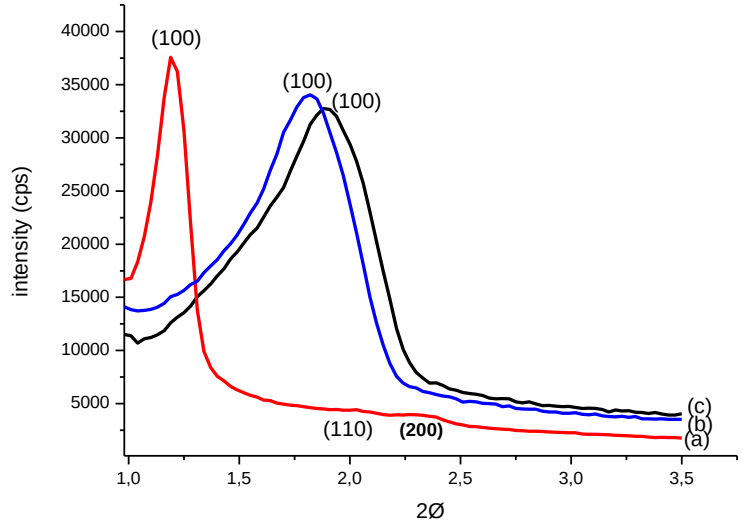

Figure 3.2.25: The PXRD patterns of silica particles obtained from the SDS-P123 system at 19^{0}C with $NaNO_3$ concentrations of (a) 0.25M, (b) 0.50M, and (c) 0.75M.

Figure 3.2.26 displays the N_2 adsorption-desorption branches of the silica particles synthesized in the presence of nitrate ion. It is noticeable that all isotherms are type-

IV, indicating that the silica particles are mesoporous. The desorption branch of the isotherm shows a characteristic type-I hysteresis path, indicating spherical, regular and open-pores.

The BJH desorption curve also indicate that the structure of the synthesized silica particles are mesoporous, see Figure 3.2.27, and the pore size distribution is quite narrow. The pore size of the synthesized particles changes from 5.0 nm to 3.2 nm when nitrate ion concentration is increased from 0.25M to 0.75M

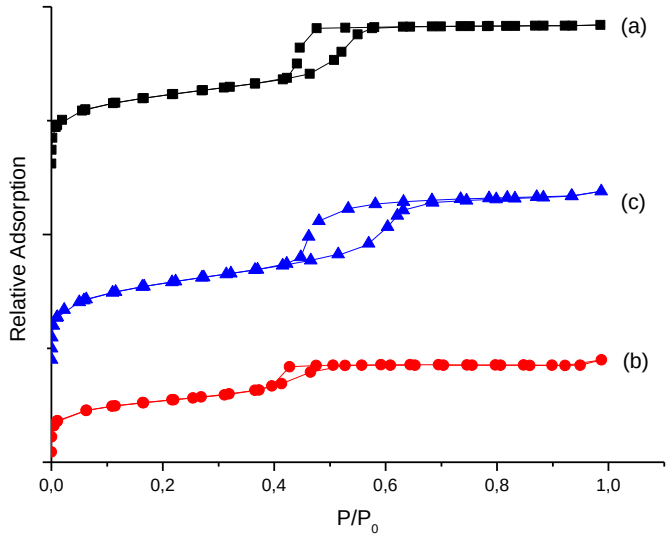

Figure 3.2.26: The N_2 adsorption-desorption isotherms (at 77K) of the silica particles obtained from the SDS-P123 system at 19^0C and $NaNO_3$ concentrations of (a) 0.25M, (b) 0.50M, and (c) 0.75M.

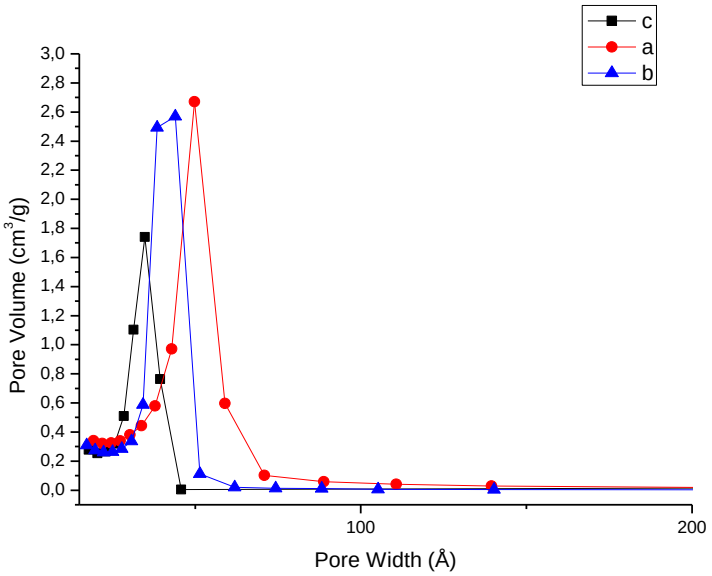

Figure 3.2.27: The BJH desorption pore size distribution (diameter) for the silica particles obtained from the SDS-P123 system at 19^0C and $NaNO_3$ concentrations of (a) 0.25M (3.5nm), (b) 0.50M (4.0nm), and (c) 0.75M (5.0nm).

CONCLUSION

In this thesis, the synthesis of mesoporous silica particles using a SDS-Pluronic system were investigated, where the pluronics are P65 and P123. The temperature and pH of the solution media and the concentration of the surfactants, mole ratio of the SDS/Pluronic, presence of alkali salts, and TMOS amount in the solution are effective on the morphology and pore structure of the silica particles.

The SDS/P65 system, which can be modified using various salts to produce mesoporous silica particles, gives microporous uniform spheres by adjusting the pH and temperature of the synthesis media. The ideal reaction temperature is in the range of 20^0C to 30^0C. pH ranges of 4.0 to 6.5 and 7.5 to 9.5 were ideal for synthesizing mono-dispersed silica spheres. Also particle size can be controlled by changing pH of the media, such that the average particle size increases linearly from 200 nm to 1000 nm by increasing pH from 4.0 to 6.0 and decreases from 1000 nm to 250 nm by increasing pH of the reaction media from 6.0 to 7.0.

In the absence of alkali salts in the reaction media, the pore structure of the particles is microporous, which results in low surface areas (between 100 m^2/g and 250 m^2/g). The mesoporous silica particles with distinct morphologies and controllable pore structures can be obtained by decreasing the solubility of P65 in the aqueous media by lowering CMC and CMT values. This can be achieved by using the anions of the Hoffmeister series. Addition of NaCl to the reaction media enhances the meso-order in the particles that have high surface areas (between 400 m^2/g and 600 m^2/g). However, addition of NaCl, results in a lost of uniformity in the morphology and increases the pore size distribution of the particles.

The understandings of the SDS-P65 system, can be used to optimize the pH and the temperature of the synthesis solution (pH 0.8-1.5 at 17^0C to 27^0C). The low CMT and CMC of P123 make this surfactant more convenient for the mesoporous silica synthesis. Playing with the parameters, the pore size, particle size, and morphology of the particles can easily be tuned. The mole ratio of SDS/P123 is effective in the aggregation and self assembly of the micelles. Therefore it is indirectly very effective on the morphologies of the silica particles. By changing the SDS/P123 mole ratio, mesostructured worm-like particles, muffin shaped and rods can be synthesized. The surface area of the particles decreases from 650 m^2/g to 450m^2/g by increasing the SDS/P123 mole ratio from 0.1 to 1.0. The pore size of the particles changed between 3.0 and 4.5 nm with changing SDS concentration.

The effects of nitrate and chloride ion have been investigated and it has been concluded that the addition of inorganic salts of these anions has effects on the morphology and meso-structure. The addition of nitrate anion causes a morphological transition, addition of small amount of $NaNO_3$ changes spherical particles to amorphous silica however at higher $NaNO_3$ concentrations muffin shaped and worm like particles can be obtained. The amount of nitrate ion also affects the pore size and wall thickness of the synthesized silica particles. By increasing the amount of nitrate ion (between 0.20M and 1.0M), the pore size of the particles can be reduced from 5.0 nm to 3.5 nm. The chloride ion has also similar effects, the addition of chloride salts cause morphological transitions, however they have small effects on the poresize.

The amount of TMOS in the reaction media is another important factor determining the morphology and meso-structure of the silica particles. At optimized conditions (SDS/P123 mole ratio of 2.0 at 19^0C pH of 1.0) the increasing amount of

TMOS results in plugged pores and disordered particles. However with the precise control of this parameter pore size can be adjusted between 3.0 and 6.0 nm.

The synthesis temperature is pivotal to synthesize mesoporous particles with distinct morphologies in the SDS-P123 system. The synthesis temperatures can be changed between 17^0C and 27^0C to observe morphological transition. The low temperatures (17-19^0C) are necessary to synthesize long mesoporous silica fibers, up to 1-2μm.

REFERANCES

1. Antonelli, D.M. and J.Y. Ying, *Mesoporous materials.* Current Opinion in Colloid & Interface Science, 1996. **1**(4): p. 523-529.
2. Davis, M.E., *Ordered porous materials for emerging applications.* Nature, 2002. **417**(6891): p. 813-821.
3. Hartmann, M., *Ordered mesoporous materials for bioadsorption and biocatalysis.* Chemistry of Materials, 2005. **17**(18): p. 4577-4593.
4. Wan, Y. and D.Y. Zhao, *On the controllable soft-templating approach to mesoporous silicates.* Chemical Reviews, 2007. **107**(7): p. 2821-2860.
5. Davis, M.E. and R.F. Lobo, *ZEOLITE AND MOLECULAR-SIEVE SYNTHESIS.* Chemistry of Materials, 1992. **4**(4): p. 756-768.
6. Corma, A., *From microporous to mesoporous molecular sieve materials and their use in catalysis.* Chemical Reviews, 1997. **97**(6): p. 2373-2419.
7. Beck, J.S., et al., *A NEW FAMILY OF MESOPOROUS MOLECULAR-SIEVES PREPARED WITH LIQUID-CRYSTAL TEMPLATES.* Journal of the American Chemical Society, 1992. **114**(27): p. 10834-10843.
8. Inagaki, S., et al., *An ordered mesoporous organosilica hybrid material with a crystal-like wall structure.* Nature, 2002. **416**(6878): p. 304-307.
9. Kramer, E., et al., *Synthesis of nanoporous silica with new pore morphologies by templating the assemblies of ionic block copolymers.* Langmuir, 1998. **14**(8): p. 2027-2031.
10. Chan, H.B.S., P.M. Budd, and T.D. Naylor, *Control of mesostructured silica particle morphology.* Journal of Materials Chemistry, 2001. **11**(3): p. 951-957.

11. Che, S., et al., *Control of crystal morphology of SBA-1 mesoporous silica.* Chemistry of Materials, 2001. **13**(7): p. 2237-+.

12. Grun, M., et al., *Novel pathways for the preparation of mesoporous MCM-41 materials: control of porosity and morphology.* Microporous and Mesoporous Materials, 1999. **27**(2-3): p. 207-216.

13. Zhao, D.Y., et al., *Morphological control of highly ordered mesoporous silica SBA-15.* Chemistry of Materials, 2000. **12**(2): p. 275-+.

14. Boissiere, C., et al., *A new synthesis of mesoporous MSU-X silica controlled by a two-step pathway.* Chemistry of Materials, 2000. **12**(10): p. 2902-2913.

15. Kresge, C.T., et al., *ORDERED MESOPOROUS MOLECULAR-SIEVES SYNTHESIZED BY A LIQUID-CRYSTAL TEMPLATE MECHANISM.* Nature, 1992. **359**(6397): p. 710-712.

16. Sayari, A. and S. Hamoudi, *Periodic mesoporous silica-based organic - Inorganic nanocomposite materials.* Chemistry of Materials, 2001. **13**(10): p. 3151-3168.

17. Ryoo, R., S.H. Joo, and J.M. Kim, *Energetically favored formation of MCM-48 from cationic-neutral surfactant mixtures.* Journal of Physical Chemistry B, 1999. **103**(35): p. 7435-7440.

18. Navrotsky, A., O. Trofymluk, and A.A. Levchenko, *Thermochemistry of Microporous and Mesoporous Materials.* Chemical Reviews, 2009. **109**(9): p. 3885-3902.

19. Soler-illia, G.J.D., et al., *Chemical strategies to design textured materials: From microporous and mesoporous oxides to nanonetworks and hierarchical structures.* Chemical Reviews, 2002. **102**(11): p. 4093-4138.

20. Smarsly, B. and M. Antonietti, *Block copolymer assemblies as templates for the generation of mesoporous inorganic materials and crystalline films.* European Journal of Inorganic Chemistry, 2006(6): p. 1111-1119.

21. Bagshaw, S.A. and I.J. Bruce, *Rapid calcination of high quality mesostructured MCM-41, MSU-X, and SBA-15 silicate materials: A step towards continuous processing?* Microporous and Mesoporous Materials, 2008. **109**(1-3): p. 199-209.

22. Vartuli, J.C., et al., *EFFECT OF SURFACTANT SILICA MOLAR RATIOS ON THE FORMATION OF MESOPOROUS MOLECULAR-SIEVES - INORGANIC MIMICRY OF SURFACTANT LIQUID-CRYSTAL PHASES AND MECHANISTIC IMPLICATIONS.* Chemistry of Materials, 1994. **6**(12): p. 2317-2326.

23. Khodakov, A.Y., et al., *Characterization of the initial stages of SBA-15 synthesis by in situ time-resolved small-angle X-ray scattering.* Journal of Physical Chemistry B, 2005. **109**(48): p. 22780-22790.

24. Monnier, A., et al., *COOPERATIVE FORMATION OF INORGANIC-ORGANIC INTERFACES IN THE SYNTHESIS OF SILICATE MESOSTRUCTURES.* Science, 1993. **261**(5126): p. 1299-1303.

25. Attard, G.S., et al., *Mesoporous platinum films from lyotropic liquid crystalline phases.* Science, 1997. **278**(5339): p. 838-840.

26. Inada, M., et al., *Microwave-assisted sol-gel process for production of spherical mesoporous silica materials.* Journal of Materials Science, 2008. **43**(7): p. 2362-2366.

27. Pang, J.B., K.Y. Qiu, and Y. Wei, *Recent progress in research on mesoporous materials I: Synthesis.* Journal of Inorganic Materials, 2002. **17**(3): p. 407-414.

28. Chen, D.H., et al., *Nonionic block copolymer and anionic mixed surfactants directed synthesis of highly ordered mesoporous silica with bicontinuous cubic structure.* Chemistry of Materials, 2005. **17**(12): p. 3228-3234.

29. Prouzet, T. and C. Boissiere, *A review on the synthesis, structure and applications in separation processes of mesoporous MSU-X silica obtained with the two-step process.* Comptes Rendus Chimie, 2005. **8**(3-4): p. 579-596.

30. Reale, E., et al., *A fluoride-catalyzed sol-gel route to catalytically active non-ordered mesoporous silica materials in the absence of surfactants.* Journal of Materials Chemistry, 2005. **15**(17): p. 1742-1754.

31. Voegtlin, A.C., et al., *F- mediated synthesis of mesoporous silica with ionic- and non-ionic surfactants. A new templating pathway.* Microporous Materials, 1997. **9**(1-2): p. 95-105.

32. Jin, Z.W., X.D. Wang, and X.G. Cui, *Acidity-dependent mesostructure transformation of highly ordered mesoporous silica materials during a two-step synthesis.* Journal of Non-Crystalline Solids, 2007. **353**(26): p. 2507-2514.

33. Demirors, A.F., M. Arslan, and O. Dag, *The effect of anions of transition metal salts on the structure of modified mesostructured silica films and monoliths.* Microporous and Mesoporous Materials, 2007. **98**(1-3): p. 249-257.

34. Ma, J.H., et al., *Salt-induced micellization of a triblock copolymer in aqueous solution: A H-1 nuclear magnetic resonance spectroscopy study.* Langmuir, 2007. **23**(6): p. 3075-3083.

35. Renoncourt, A., et al., *Specific alkali cation effects in the transition from micelles to vesicles through salt addition.* Langmuir, 2007. **23**(5): p. 2376-2381.

36. Su, Y.L., et al., *Study of salt effects on the micellization of PEO-PPO-PEO block copolymer in aqueous solution by FTIR spectroscopy.* Langmuir, 2002. **18**(3): p. 865-871.

37. Sierra, L., et al., *Templating behavior of a triblock copolymer surfactant with very long hydrophilic PEO chains (PEO140PPO39PEO140) for the synthesis of cubic mesoporous silica with large cage-like cavities.* Microporous and Mesoporous Materials, 2008. **113**(1-3): p. 352-361.

38. Trong, L.C.P., M. Djabourov, and A. Ponton, *Mechanisms of micellization and rheology of PEO-PPO-PEO triblock copolymers with various architectures.* Journal of Colloid and Interface Science, 2008. **328**(2): p. 278-287.

39. Zhou, Z. and B. Chu, *PHASE-BEHAVIOR AND ASSOCIATION PROPERTIES OF POLY(OXYPROPYLENE)-POLY(OXYETHYLENE)-POLY(OXYPROPYLENE) TRIBLOCK COPOLYMER IN AQUEOUS-SOLUTION.* Macromolecules, 1994. **27**(8): p. 2025-2033.

40. Imperor-Clerc, M., P. Davidson, and A. Davidson, *Existence of a microporous corona around the mesopores of silica-based SBA-15 materials templated by triblock copolymers.* Journal of the American Chemical Society, 2000. **122**(48): p. 11925-11933.

41. Jin, Z.W., X.D. Wang, and X.G. Cui, *Synthesis and morphological investigation of ordered SBA-15-type mesoporous silica with an amphiphilic triblock copolymer template under various conditions.* Colloids and Surfaces a-Physicochemical and Engineering Aspects, 2008. **316**(1-3): p. 27-36.

42. Kim, J.H., et al., *Synthesis of monodisperse silica spheres with solid core and mesoporous shell: Morphological control of mesopores.* Colloids and Surfaces a-Physicochemical and Engineering Aspects, 2008. **313**: p. 77-81.

43. Naik, S.P. and I. Sokolov, *Room temperature synthesis of nanoporous silica spheres and their formation mechanism.* Solid State Communications, 2007. **144**(10-11): p. 437-440.

44. Bakshi, M.S., et al., *Mixed-micelle formation by strongly interacting surfactant binary mixtures: effect of head-group modification.* Colloid and Polymer Science, 2002. **280**(11): p. 990-1000.

45. Flodstrom, K., H. Wennerstrom, and V. Alfredsson, *Mechanism of mesoporous silica formation. A time-resolved NMR and TEM study of silica-block copolymer aggregation.* Langmuir, 2004. **20**(3): p. 680-688.

46. Gao, C.B., et al., *Formation mechanism of anionic surfactant-templated mesoporous silica.* Chemistry of Materials, 2006. **18**(16): p. 3904-3914.

47. Jain, N.J., et al., *Salt induced micellization and micelle structures of PEO/PPO/PEO block copolymers in aqueous solution.* Colloids and Surfaces a-Physicochemical and Engineering Aspects, 2000. **173**(1-3): p. 85-94.

48. Linse, P., *MICELLIZATION OF POLY(ETHYLENE OXIDE)-POLY(PROPYLENE OXIDE) BLOCK-COPOLYMERS IN AQUEOUS-SOLUTION.* Macromolecules, 1993. **26**(17): p. 4437-4449.

49. Yano, K. and T. Nakamura, *Synthesis of highly monodispersed core/shell mesoporous silica spheres.* Chemistry Letters, 2006. **35**(9): p. 1014-1015.

50. Alexandridis, P. and T.A. Hatton, *POLY(ETHYLENE OXIDE)-POLY(PROPYLENE OXIDE)-POLY(ETHYLENE OXIDE) BLOCK-COPOLYMER SURFACTANTS IN AQUEOUS-SOLUTIONS AND AT INTERFACES - THERMODYNAMICS, STRUCTURE, DYNAMICS, AND MODELING.* Colloids and Surfaces a-Physicochemical and Engineering Aspects, 1995. **96**(1-2): p. 1-46.

51. Alexandridis, P., T. Nivaggioli, and T.A. Hatton, *TEMPERATURE EFFECTS ON STRUCTURAL-PROPERTIES OF PLURONIC P104 AND F108 PEO-PPO-PEO BLOCK-COPOLYMER SOLUTIONS.* Langmuir, 1995. **11**(5): p. 1468-1476.

52. Yang, L. and P. Alexandridis, *Polyoxyalkylene block copolymers in formamide-water mixed solvents: Micelle formation and structure studied by small-angle neutron scattering.* Langmuir, 2000. **16**(11): p. 4819-4829.

53. Das, C., et al., *Mixed micellization of anionic-nonionic surfactants in aqueous media: a physicochemical study with theoretical consideration.* Colloid and Polymer Science, 2008. **286**(10): p. 1143-1155.

54. Herrington, K.L., et al., *PHASE-BEHAVIOR OF AQUEOUS MIXTURES OF DODECYLTRIMETHYLAMMONIUM BROMIDE (DTAB) AND SODIUM DODECYL-SULFATE (SDS).* Journal of Physical Chemistry, 1993. **97**(51): p. 13792-13802.

55. Goldmints, I., et al., *Small-angle neutron scattering study of PEO-PPO-PEO micelle structure in the unimer-to-micelle transition region.* Langmuir, 1997. **13**(14): p. 3659-3664.

56. Mesa, M., L. Sierra, and J.L. Guth, *Contribution to the study of the formation mechanism of mesoporous SBA-15 and SBA-16 type silica particles in aqueous acid solutions.* Microporous and Mesoporous Materials, 2008. **112**(1-3): p. 338-350.

57. Mesa, M., L. Sierra, and J.L. Guth, *Contribution to the study of the formation mechanism of mesoporous silica type SBA-3.* Microporous and Mesoporous Materials, 2007. **102**(1-3): p. 70-79.

58. Mou, C.Y. and H.P. Lin, *Control of morphology in synthesizing mesoporous silica.* Pure and Applied Chemistry, 2000. **72**(1-2): p. 137-146.

59. Ganguly, R., et al., *Effect of SDS on the self-assembly behavior of the PEO-PPO-PEO triblock copolymer (EO)(20)(PO)(70)(EO)(20).* Journal of Physical Chemistry B, 2006. **110**(20): p. 9843-9849.

60. Ortona, O., et al., *Interaction between cationic, anionic, and non-ionic surfactants with ABA block copolymer Pluronic PE6200 and with BAB reverse block copolymer Pluronic 25R4.* Journal of Colloid and Interface Science, 2006. **301**(1): p. 63-77.

61. Bharatiya, B., et al., *The effects of salts and ionic surfactants on the micellar structure of tri-block copolymer PEO-PPO-PEO in aqueous solution.* Journal of Dispersion Science and Technology, 2008. **29**(5): p. 696-701.

62. Attard, G.S., J.C. Glyde, and C.G. Goltner, *LIQUID-CRYSTALLINE PHASES AS TEMPLATES FOR THE SYNTHESIS OF MESOPOROUS SILICA.* Nature, 1995. **378**(6555): p. 366-368.

63. Burkett, S.L., S.D. Sims, and S. Mann, *Synthesis of hybrid inorganic-organic mesoporous silica by co-condensation of siloxane and organosiloxane precursors.* Chemical Communications, 1996(11): p. 1367-1368.

64. Poyraz, A.S., *Synthesıs of Mesoporous Silica Particles by Controllıng the CTABR-Pluronic Assembly*, in *Chemistry*. 2009, Bilkent: Ankara.

65. Poyraz, A.S., C. Albayrak, and O. Dag, *The effect of cationic surfactant and some organic/inorganic additives on the morphology of mesostructured silica templated by pluronics.* Microporous and Mesoporous Materials, 2008. **115**(3): p. 548-555.

66. Poyraz, A.S. and O. Dag, *Role of Organic and Inorganic Additives on the Assembly of CTAB-P123 and the Morphology of Mesoporous Silica Particles.* Journal of Physical Chemistry C, 2009. **113**(43): p. 18596-18607.

67. Galarneau, A., et al., *Kinetics of formation of micelle-templated silica mesophases monitored by electron paramagnetic resonance.* Journal of Colloid and Interface Science, 1998. **201**(2): p. 105-117.

68. Ottaviani, M.F., et al., *EPR investigations on the formation of micelle-templated silica.* Microporous and Mesoporous Materials, 2001. **44**: p. 1-8.

69. Cui, X.H., et al., *Mechanism of the Mixed Surfactant Micelle Formation.* Journal of Physical Chemistry B. **114**(23): p. 7808-7816.

70. Misselyn-Bauduin, A.M., et al., *Mixed micelles of anionic-nonionic and anionic-zwitterionic surfactants analyzed by pulsed field gradient NMR.* Langmuir, 2000. **16**(10): p. 4430-4435.

71. Stein, A., *Sphere templating methods for periodic porous solids.* Microporous and Mesoporous Materials, 2001. **44**: p. 227-239.

72. Trewyn, B.G., et al., *Mesoporous silica nanoparticle based controlled release, drug delivery, and biosensor systems.* Chemical Communications, 2007(31): p. 3236-3245.

73. Yang, H.F., et al., *One-step synthesis of highly ordered mesoporous silica monoliths with metal oxide nanocrystals in their channels.* Advanced Functional Materials, 2005. **15**(8): p. 1377-1384.

74. Yu, C.Z., et al., *Nonionic block copolymer synthesis of large-pore cubic mesoporous single crystals by use of inorganic salts.* Journal of the American Chemical Society, 2002. **124**(17): p. 4556-4557.

75. Benrraou, M., B.L. Bales, and R. Zana, *Effect of the nature of the counterion on the properties of anionic surfactants. 1. Cmc, ionization degree at the cmc and aggregation number of micelles of sodium, cesium, tetramethylammonium, tetraethylammonium, tetrapropylammonium, and tetrabutylammonium dodecyl sulfates.* Journal of Physical Chemistry B, 2003. **107**(48): p. 13432-13440.

76. Cacace, M.G., E.M. Landau, and J.J. Ramsden, *The Hofmeister series: salt and solvent effects on interfacial phenomena.* Quarterly Reviews of Biophysics, 1997. **30**(3): p. 241-277.

77. Zhang, L.F. and A. Eisenberg, *Morphogenic effect of added ions on crew-cut aggregates of polystyrene-b-poly(acrylic acid) block copolymers in solutions.* Macromolecules, 1996. **29**(27): p. 8805-8815.

78. Thommes, M., et al., *Adsorption hysteresis of nitrogen and argon in pore networks and characterization of novel micro- and mesoporous silicas.* Langmuir, 2006. **22**(2): p. 756-764.